UNIVERSITY OF NAPLES "FEDERICO II"

DOCTORATE SCHOOL IN
MOLECULAR MEDICINE AND MEDICAL BIOTECHNOLOGY
XXX CYCLE

DNA Methylation of CDKN2A-B suppressor genes: mechanism and consequences

TUTOR

Prof. Vittorio Enrico Avvedimento

CANDIDATE

Francesca Ludovica Boffo

PHD COORDINATOR
Prof. Vittorio Enrico Avvedimento

ACADEMIC YEAR 2016-2017

To us…

Because our friendship was the most

successful experiment.

DNA Methylation Of CDKN2A-B Suppressor Genes: Mechanism And Consequences

TABLE OF CONTENTS

LIST OF ABBREVIATIONS **5**

ABSTRACT **6**

1. INTRODUCTION **7**
1.1 CYCLIN-DEPENDENT KINASE INHIBITORS 7
1.2 SENESCENCE IS A BARRIER TO TRANSFORMATION 10
1.3 DNA METHYLATION AND SILENCING OF INK4-ARF LOCUS 11
1.4 METHYLATION AND CANCER PROGRESSION 13

2 AIM OF THE STUDY **15**

3 MATERIAL AND METHODS **16**
3.1 CELL CULTURE AND DRUG TREATMENTS 16
3.2 DNA AND RNA EXTRACTION 16
3.3 cDNA AND REAL TIME PCR 16
3.4 PROTEIN EXTRACTION AND WESTERN BLOT ANALYSIS 17
3.5 CHROMATIN IMMUNOPRECIPITATION 17
3.6 FLOW CYTOMETRY ANALYSIS 17
3.7 MeDIP ASSAY 18
3.8 BISULFITE TREATMENT AND AMPLICON LIBRARY PREPARATION 18
3.9 WHOLE EXOME SEQUENCING 19
3.10 SEQUENCE ANALYSIS 19
3.11 ANTIBODIES 19
3.12 STATISTICAL ANALYSIS 19

4 RESULTS **21**
4.1 TRANSCRIPTIONAL REGULATION OF INK4-ARF LOCUS GENES DURING CELL CYCLE 21
4.2 DNA DAMAGE SIGNATURES AT CDKN2A-B GENE PROMOTERS. 24
4.3 INHIBITION OF DNA POLYMERASE OR RNA POLYMERASE REDUCES γH2AX ACCUMULATION AT CDKN2A-B PROMOTERS 26
4.4 METHYLATION ASSOCIATED WITH DNA DAMAGE AT $p16^{INK4A}$ PROMOTER 27
4.5 METHYLATED CDKN2A ALLELES IN VIVO EVOLVE DURING THE PROGRESSION OF ACUTE MYELOID LEUKEMIA 28

5 DISCUSSION **34**
5.1 MOLECOLAR COLLISIONS BETWEEN REPLICATION AND TRANSCRIPTION MACHINES ARE THE SOURCE OF DNA DAMAGE 34
5.2 DNA DAMAGE AND DNA METHYLATION 35
5.3 METHYLATION OF CDKN2A-B SUPPRESSOR GENES IS A FREQUENT EVENT DURING NEOPLASTIC PROGRESSION 35
5.4 DNA METHYLATION AS A BAR-CODE TO IDENTIFY AND TRACK SPECIFIC EPIALLELES 36

6 CONCLUSIONS **39**

7 REFERENCES **40**

LIST OF ABBREVIATIONS

5-AzadC	5-Aza-2-deoxycytidine
AMA	Alpha amanitin
AML	Acute myeloid leukemia
APDH	Aphidicolin
ARF	Alternative reading frame
BER	Base excision repair
BM	Bone marrow
CDKI	Cyclin-dependent kinase inhibitor
CDKN	Cyclin-dependent kinase inhibitor
CDS	Coding DNA sequences
CFS	Common fragile sites
ChIP	Chromatin immunoprecipitation
DMSO	Dimethyl sulfoxide
DNMT	DNA methyltransferase
DSB	Double strand break
ES	Embryonic stem (cells)
FBS	Fetal bovine serum
GEMMs	Genetically engineered mouse models
GFP	Green fluorescent protein
HeLa	Immortalized cervical cancer cells
HR	Homologous recombination
iPS	Induced Pluripotent Stem cells
LOH	Loss of heterozygosity
MDS	Myelodysplastic syndrome
MeDIP	Methylated DNA immunoprecipitation
mRNA	Messenger RNA
ORC	Origin Recognition Complex
ORi	Origin of Replication
PCNA	Proliferating cell nuclear antigen
PcG	Polycomb-group proteins
qPCR	Quantitative Polymerase Chain Reaction
Rb	Retinoblastoma
RFP	Replication Fork Pause
RNA	Ribonucleic Acid
SNP	Single Nucleotide Polymorphism
TGF-β	Transforming growth factor beta
TSS	Transcription Start Site
αSMA	Alpha Smooth Muscle Actin

ABSTRACT

Tumor suppressor genes, $p15^{INK4B}$ and $p16^{INK4A}$ p14ARF, are the most frequently silenced genes in human cancers (Kim and Sharpless, 2006) because they represent a biological barrier to transformation (Skalska *et al.,* 2013). Frequently, silencing is the result of DNA methylation of promoter regions, and to date, the precise mechanism is not known.
Here, we present evidence that DNA methylation is associated with DNA damage caused by collisions between DNA and RNA polymerases near the transcription start sites. Inhibition of replication or transcription greatly reduces DNA damage and ultimately, local CpG methylation.
This mechanism generates *in vivo* many variants (alleles) of $p15^{INK4B}$ $p16^{INK4A}$ and p14ARF genes, which differ only by the occurrence of methylated CpG within the sequence (epialleles). If some epialleles are positively selected, we expect to find them amplified in a complex population of proliferating cells. We have tested this notion by systematically investigating: 1. the configuration of methylated CpGs in each $p16^{INK4A}$ sequenced molecule (epiallele) and; 2. the frequency of families of epialleles during the progression of acute myeloid leukemia (AML) in cells from the bone marrow or the blood of three patients.

The relevant results can be summarized as follows: 1. The epialleles, defined by unique methylation profiles, were stable and patient-specific. 2. The epialleles displayed gene specific methylation signatures and were somatically inherited; 3. Some epialleles were eliminated by the demethylating therapy (5-AzadC, Vidaza®), others were resistant or amplified by the demethylating drug and their frequency increased before and during the disease relapse; 4. The presence of high levels of epialleles after the therapy predicted the chemoresistance; 5. The epialleles of another suppressor, p21/WAF, in the same patients, did not evolve and remained stable throughout the progression of the disease; 6. Specific $p16^{INK4A}$ gene CpGs function as “seeds” for further methylation.

Collectively, these data indicate: 1. An epigenetic mechanism driving the evolution of AML by dynamic methylation of alleles of $p16^{INK4A}$ suppressor gene; 2. The methylation changes during AML progression may be facilitated by DNA damage; 3. The distribution and the frequency of families of $p16^{INK4A}$ epialleles overtime accurately describe the evolution of myeloid acute leukemia.

1. INTRODUCTION

1.1 CYCLIN-DEPENDENT KINASE INHIBITORS

1.1.1 MEMBERS AND THEIRE FUNCTION

Cyclin dependent kinase inhibitors (CDKIs) are proteins involved in the control of cell cycle progression. They inhibit the enzymatic activity of cyclin-dependent kinase (CDK) by binding.
CDKIs are divided into two major groups on the basis of their structural characteristics and specificity of binding.
One is composed by INK4 (inhibitor of CDK4) family comprising $p16^{INK4A}$ $p15^{INK4B}$ $p18^{INK4C}$ $p19^{INK4D}$, which inhibit the complex cyclin D-CDK4/6 (Sànchez-Beato *et al.,* 1997). The other family, Cip/Kip, is composed by $p21^{CIP1/WAF1}$ $p27^{KIP1}$ $p57^{KIP2}$ which inhibit a broad spectrum of cyclin-CDK complexes (Starostina and Kipreos, 2012).

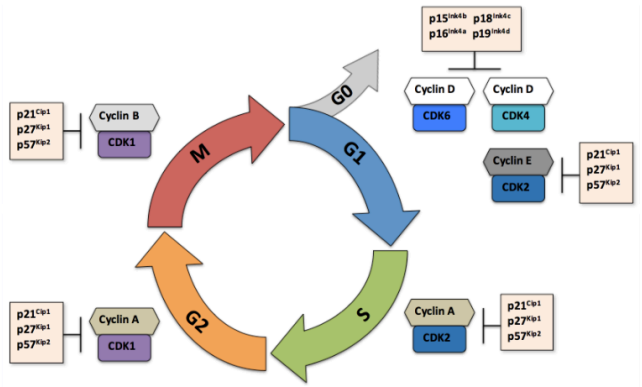

Figure 1: Cell Cycle Progression. CDK and cyclins promote the progression through the cell cycle**.** Different CDKIs are expressed at different phases of the cell cycle.

The expression of these genes is frequently inhibited in human cancers. Promoter hypermethylation, point mutations, deletion are responsible for silencing of these genes in more than 90% of human cancers. In the last decades, researchers are focusing their attention on cell cycle regulators as targets for the development of new molecules to cure cancer (Otto and Sicinski, 2017).

1.1.2 INK4 FAMILY MEMBERS

INK4 family members are highly conserved in evolution and are involved in cell cycle control at different levels.
$p15^{INK4B}$and $p16^{INK4A}$ act as peculiar CDK4/6 inhibitors in the retinoblastoma pathway; their inactivation allows cells to escape the G1 restriction point in the cell cycle (Ferreira *et al.,* 2015). $p19^{INK4D}$ binds and promotes MDM2 degradation, a protein involved in retinoblastoma and p53 pathways (Zhang *et al.,* 1998).
The INK4 family members are clustered in a small region of chromosome 9 (9p21) (Fig. 2). The unusual evolution of this locus can be explained by the advantage to coordinate the transcriptional regulation of several cell cycle regulators clustered in the same DNA segment with the same chromatin-remodeling events. Repression by Polycomb (PcG) complexes is one way to silence the genes in the INK4 locus through the induction of local H3K27methylation. Loss of PcG genes reveals a defect in hematopoiesis and other disorders in part due to de-repression of INK4/Arf locus (Gil and Peters, 2006). If silencing INK4 genes is a rather simple process, their positive regulation is rather complex, since it is controlled by different agents, which act on different members of the gene family. Ionizing radiation, DNA damage (Lafargue *et al.,* 2017), ultraviolet irradiation, oxidative stress response (Jenkins *et al.,* 2011), replicative senescence (Helman *et al.,* 2016) activate INK4a. Mitogen agents such as RAS and MYC proteins activate both INK4a and ARF (Gil and Peters, 2006) while INK4b activation depends mostly on Transforming growth factor β (TGFβ) signaling (Rich *et al.,* 1999).

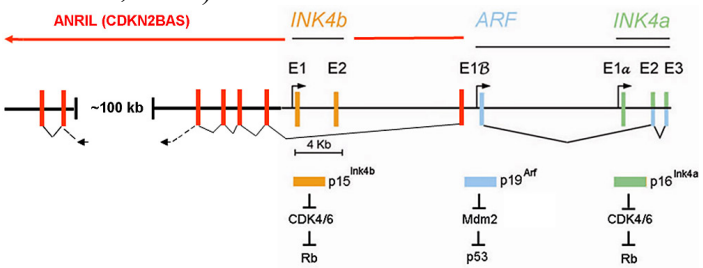

Figure 2: Schematic Representation Of INK4-ARF Locus. Bar (colored vertical lines) indicates coding exons of the genes separated by introns (horizontal black lines). Exons E1 and E2 of INK4a (light green) are translated in an alternative reading frame in order to synthesize p19ARF or p14ARF human protein. INK4a-b genes suppress CDK4/6 to activate Retinoblastoma (Rb) pathway and inhibit cell cycle progression; p14ARF directly suppresses Mdm2 to activate p53 and negatively regulates cell cycle progression. ANRIL is a long non-coding RNA transcribed from an undefined promoter in an antisense direction relative to INK4-ARF genes. Its products are spliced and putative exons indicated by the red bar.
Adapted from Sherr, C. J. 2012. 1:731-741.

1.1.3 CIP/KIP FAMILY MEMBERS

Cip/Kip family members act at the G1/S and G2/M checkpoints. Initially, all family members were considered negative regulators of the cell cycle (Harper *et al.,* 1993). Eventually, new data demonstrated that cytoplasmic p21 and p27 were also able, in contrast with their nuclear role, to mediate the assembly and nuclear import of CDK4/6-cyclin D (Cheng *et al.,* 1999). Therefore, p21 and p27 activity is influenced by their localization.

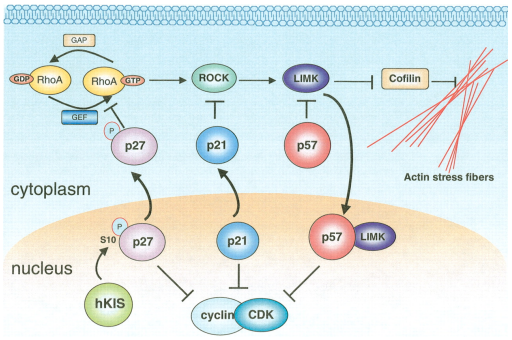

Figure 3: Different Action Mediated By CIP/KIP Family Members in the Nucleus and in the Cytoplasm. In the nucleus CIP/KIP family members act as cyclin-CDK inhibitors, while in the cytoplasm they regulate actin reorganization by inhibiting Rho-Rock-Limk pathway. The mechanism underlying p21 export to the cytoplasm is still unknown. p57 inhibits the function of LIMK preventing its binding to cofilin.
Adapted from Denicourt 2004;18(8):851-5.

Overall, these genes are involved in the control of cell proliferation during development, differentiation and response to different types of cellular stresses. However, selective pathways activate each member of the family.
The p21 protein, for example, is a well-characterized transcriptional target of p53 and it mediates DNA damage-induced cell cycle arrest in G1 and G2 (Gartel and Tyner, 1999). On the other hand, p27 maintains the cells in a quiescent state. Cell cycle is accompanied by down-regulation of the protein (Gartel and Radhakrishnan, 2005). Also, p57 influences embryonic development.
In conclusion, the Cip/Kip family members are essential for cell growth and survival, because knockout mouse models for each member show increase of body size and hyperplasia or delayed differentiation (Besson *et al.,* 2008).

1.1.4 THE INK4 LOCUS AFFECTS CELL FATE

INK4/Arf locus encodes three potent inhibitors of proliferation. Silencing of the locus is required to induce pluripotent stem cells (iPS) or to support proliferation of embryonic stem (ES) cells (Li et al., 2009). On the other hand, p16Ink4a protein is a well-known biomarker of aging in mammalian cell. Accelerated aging can be rescued in T or B lymphocytes by a deletion of p16Ink4a; however, it should be pointed out that loss p16Ink4a leads to B-cell neoplasia (Liu et al., 2011). Methylation of INK4/Arf locus is found in several human cancers (Serrano et al., 1996). Also, germ line mutations of p16INK4a are associated with malignant melanoma and pancreatic cancer (Whelan et al., 1995). Taken together, these data suggest that CDKN2A/B genes are involved in the modulation of the cell life balance: proliferation or senescence. Overexpression or down-regulation of these genes can result in cellular death or exit from the cycle. While CDKN2A/B overexpression commits cells to premature aging, down-regulation of the expression of these genes promotes cancer progression and acquisition of immortality (LaPak and Burd, 2014). The expression of INK4/Arf locus genes acts as a barrier to transformation by preventing the progression of damaged DNA harboring cells into the replication process. This inhibits the spreading of deregulation and damage to daughter cells. This circuitry is the main barrier to transformation of a cell. Only cells that inhibit the expression of INK4/Arf locus genes are able to escape apoptosis and exit from the cell cycle (senescence). Since CDKN2A/B genes are clustered, damage occurring at the INK4 locus may deregulate most or all of them in few steps, providing to a normal cell the chance to overcome the damage and become immortal (Sherr, 2012).

1.2 THE SENESCENCE IS A BARRIER TO TRANSFORMATION

Senescence in humans and mice

Mice and humans have in common systemic physiology, the number of organs, many genes and this is the reason why in science mouse models are extensively used to study human diseases (Demetrius, 2005). However there is substantial evidence that cancer is driven by different signaling pathways in humans and mice.
The human life spans is 30-50 time longer than mice, suggesting that human cells undergo about 10^5 cell divisions compared to the mouse. Since the chance to develop a tumor is positively correlated to the number of mitotic

divisions, humans should have higher incidence of cancer compared to mice. This notion does not reflect the reality.
Humans and mice differ in cancer susceptibility, spectrum of age related cancer, telomere length, ability to undergo spontaneous cells immortalization. These differences derive from different pathways implicated in cellular immortalization. Mouse embryonic fibroblasts, *in vitro*, became immortalized spontaneously once telomerase activity decreases, indicating this event as the major responsible for transformation. Human fibroblasts instead, *in vitro*, after a definite number of replications, enter a phase called replicative senescence. During this phase telomerase activity decreases and the telomere became shorter, activating a DNA damage response (DDR). A single surviving clone can emerge at low frequency and eventually can became immortal. In conclusion, human cells have to cross two barriers (senescence and telomere shortening) before becoming immortalized. In humans, the driver gene of senescence is $p16^{INK4A}$; $p16^{INK4A}$ silencing and inactivation provide a proliferative selective advantage and permit the exit from senescence (Rangarajan and Weinber, 2003).

1.3 DNA METHYLATION AND SILENCING OF INK4-ARF LOCUS GENES

1.3.1 INK4-ARF LOCUS SILENCING IN HUMAN AND MOUSE

Down regulation of tumor suppressor genes is a prerequisite for cancer progression (Lee and Muller, 2010). The loss of one allele does not necessary indicate a pre-cancerous condition. The biological phenomenon called "loss of heterozygosity" (LOH) is responsible for the inactivation of the remaining copy of tumor suppressor genes and this event is a prerequisite for cancer development and/or progression. It can occur by mitotic non-disjunction or/and duplication (Thiagalingam *et al.,* 2001); mitotic recombination (Luo *et al.,* 2000); gene conversion (Zhang *et al.,* 2006); point mutation and allele deletion (Miyake *et al.,* 1994) and silencing (Kazanets *et al.,* 2016).
Gene promoter hypermethylation and silencing are common events leading to dys-regulation of gene expression in human cancers. Several studies reported a large number of human genes regulated by DNA methylation; the table below shows some examples.

Gene	*Function*	*Location*	*Tumor profile*	*Consequences*
$p16^{INK4a}$	Cyclin-dependent Kinase Inhibitor	9p21	Multiple Types	Entrance in Cell Cycle
$p14^{ARF}$	*MDM2* inhibitor	9p21	Colon, Stomach, Kidney	Degradation of *p53*
$p15^{INK4b}$	Cyclin-dependent Kinase Inhibitor	9p21	Leukemia	Entrance in Cell Cycle
hMLH1	DNA mismatch repair	3p21.3	Colon, Endometrium, Stomach	Frameshift Mutations
MGMT	DNA repair of 06-alkyl-guanine	10q26	Multiple Types	Mutations, Chemosensitivity
GSTP1	Conjugation to Glutathione	11q13	Prostate, Breast, Kidney	Adduct Accumulation?
BRCA1	DNA Repair, Transcription	17q21	Breast, Ovary	Double Strand-Breaks?
p73	p53 Homologue	1p36	Lymphoma	Unknown (Cisplatin?)
LKB1/STK11	Serine/Threonine Kinase	19p13.3	Colon, Breast, Lung	Unknown
ER	Estrogen Receptor	6q25.1	Breast	Hormone Insensitivity
PR	Progesterone Receptor	11q22	Breast	Hormone Insensitivity
AR	Androgen Receptor	Xq11	Prostate	Hormone Insensitivity
RARβ2	Retinoic Acid Receptor β2	3p24	Colon, Lung, Head and Neck	Vitamin Insensitivity?
RASSF1	Ras Effector Homologue	3p21.3	Multiple Types	Unknown
VHL	Ubiquitin Ligase Component	3p25	Kidney, Hemangioblastoma	Loss of hypoxic response?
Rb	Cell Cycle Inhibitor	13q14	Retinoblastoma	Entrance in Cell Cycle
THBS-1	Thrombospondin-1, Anti-angiogenic	15q15	Glioma	Neovascularization
CDH1	E-cadherin, cell adhesion	16q22.1	Breast, Stomach, Leukemia	Dissemination
HIC-1	Transcription Factor	17p13.3	Multiple Types	Unknown
APC	Inhibitor of β-catenin	5q21	Aerodigestive Tract	Activation β-catenin Route
COX-2	Cyclooxigenase-2	1q25	Colon, Stomach	Antinflamatory Resistance?
SOCS-1	Inhibitor of JAK/STAT Pathway	16p13.13	Liver	JAK2 Activation
SRBC	*BRCA1*-binding Protein	1p15	Breast, Lung	Unknown
SYK	Tyrosine Kinase	9q22	Breast	Unknown
RIZ1	Histone/Protein Methyltransferase	1p36	Breast, Liver	Aberrant Gene Expression?
CDH13	H-cadherin, cell adhesion	16q24	Breast, Lung	Dissemination?
DAPK	Pro-apoptotic	9q34.1	Lymphoma, Lung, Colon	Resistance to Apoptosis
TMS1	Pro-apoptotic	16p11	Breast	Resistance to Apoptosis
TPEF/HPP1	Transmembrane Protein	2q33	Colon, Bladder	Unknown

Table I: Selected Genes That Undergo CpG Island Hypermethylation In Human Cancer.
Adapted from Esteller 2002;21(35):5427-40.

Genetically engineered mouse models (GEMMs) are extensively used to study human cancer biology, but they cannot be always compared to human cancer.

Specific CpG island methylation patterns characterize different types of tumor genes in humans. There is a substantial difference in some CpG islands methylation patterns of genes involved in cancer progression between humans and GEMMs. In the Eμ-Myc mouse model of Burkitt lymphoma was reported higher DNA methylation due to high expression of DNMT3B7, a truncated isoform of DNMT3B, but this trait is not cancer specific (Shah *et al.,* 2010).

DNA promoter hypermethylation in cancer mouse cells induced by a previous inflammatory state better describes human tumorigenesis than examples in GEMMs induced-phenotypes driven by oncogenes (Diede *et al.,* 2013).

Nowadays the number of silenced human genes by promoter hypermethylation is still growing, but the mechanism is still unknown.

1.3.2 INK4-ARF LOCUS SILENCING IS A COMMON EVENT IN ACUTE LEUKEMIA

The negative regulation of cell cycle mediate by $p^{15INK4B}$ and $p16^{INK4A}$ $p14^{ARF}$ in physiological condition is the reason explaining the high rate of silencing of these genes during cancer progression (Christiansen et al., 2003).
The $p15^{INK4B}$ gene is an effector of antimitotic signaling induced by TGF-β, which is involved in the regulation of hematopoiesis. Specifically, in the myeloid lineage $p15^{INK4B}$ expression cannot be detected in $CD34^{+}$ progenitor cells but only during terminal differentiation to granulocyte (Teofili *et al.,* 2001). The $p16^{INK4A}$ gene, in an opposite trend, is expressed in $CD34^{+}$ cells, but suppressed during the terminal differentiation of the myeloid lineage (Furukawa *et al.,* 2000).
Point mutations are rare in hematopoietic diseases, while homozygous deletion or gene silencing by promoter hypermethylation at CpG sites are common events, especially in acute myeloid leukemia and in myelodysplastic syndrome (Drexler, 1998). These abnormalities are considered as early events in leukemogenesis (Christiansen *et al.,* 2003). Both, $p15^{INK4B}$ and $p16^{INK4A}$ genes are silenced in leukemia, $p15^{INK4B}$ promoter is hypermethylated during the initial steps of cancer progression, while $p16^{INK4A}$ gene methylation is acquired later, during clonal evolution (Chim *et al.,* 2001).

1.4 DNA METHYLATION AND CANCER PROGRESSION

1.4.1 GENETIC AND EPIGENETIC CHANGES IN CANCER

Cancer is the result of genomic imbalance and epigenetic modifications leading to cell immortalization.
A common characteristic of genetic and epigenetic modifications is their hereditability. Genetically and epigenetically-modified somatic cells can transfer the information to daughter cells which acquire the ability to expand to one or more clones, which are positively selected by their high replication rate (Sadikovic *et al.,* 2008).

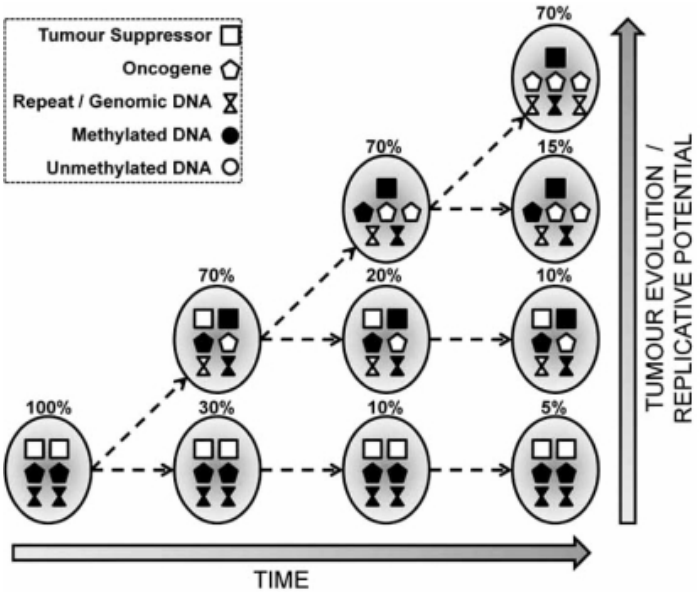

Figure 4: Co-evolution Of Genetic And Epigenetic Changes. Genetic and epigenetic changes together increase the potential and drive tumor evolution.
Adapted from Sadikovic et al., 2008;doi:10.2174/138920208785699580.

1.4.2 THE EPIGENOME PLAYS A KEY ROLE IN CANCER EVOLUTION

Tumor heterogeneity is one of the main causes of failure of cancer therapies, and chemo-resistance. Tumor progression is a dynamic event driven by genetic and epigenetic modifications in somatic cells (Urbach *et al.,* 2012). Is still unknown the cause-effect relationship between genetic and epigenetic modification during cancer progression, however it is a fact that the same genetic mutation may cause different phenotypes (Li *et al.,* 2016).
DNA methylation, as stable and inherited epigenetic trait, is extremely polymorphic in somatic cells and is generated by alleles differing only for the location of methylated CpGs. These variants are named epialleles.
These epialleles are polymorphic and may represent a "cellular barcode" that can be used to track specific cells in complex populations (Landan *et al.,* 2012; Russo et al., 2016).

2.

3. AIM OF THE STUDY

Cancer is a dynamic disease. During neoplastic progression, tumor cells gain mutations and modify their epigenetic profiles to increase their fitness. Epigenetic and genetic clonal heterogeneity is tightly associated with chemoresistance and evolution of tumor cells.
The progressive silencing of $p15^{INK4B}$ and $p16^{INK4A}$ p14ARF oncosoppressor genes confers a selective advantage to tumor cells as shown by the high frequency of transcriptional inactivation of these genes in most types of cancer.

The main goals of this study are:
-The mechanism(s) responsible for the high frequency of methylation of $p15^{INK4B}$ and $p16^{INK4A}$ p14ARF suppressor genes.
-The analysis of methylated alleles of $p16^{INK4A}$ during evolution of acute myeloid leukemia in human patients.

3. MATERIAL AND METHODS

3.1 CELL CULTURE AND DRUGS TREATHMENT

HeLa cells were cultured in DMEM medium with 4,5g/L D-glucose and Pyruvate (Gibco, Carlsbad, CA, USA) complemented with 100u/mL of penicillin and 100μg/mL of streptomycin (Gibco, Carlsbad, CA, USA), 2mM L-glutamine (Gibco, Carlsbad, CA, USA), in presence or absence of 10% of FBS (South America origin, Brazil, Invitrogen, Rockville, MD, USA). All culture were maintained in 37 °C at 5% CO_2 humidified atmosphere.
All drugs treatment were administered to adherent cells and dissolved in complete or medium without FBS.
Aphidicolin (Sigma-Aldrich, St Louis, MO, USA) at final concentration of 1μg/mL and α-amanitine (Sigma-Aldrich, St Louis, MO, USA) at final concentration of 2,5μM, were added to cell culture medium. Etoposide (Sigma-Aldrich, St Louis, MO, USA) was added to cells culture medium for 30 minutes at 25μM final concentration.

3.2 DNA AND RNA EXTRACTION

DNA was extracted from cell pellets, purified by phenol/chloroform/isoamyl alcohol extraction and precipitated by ethanol. The pellet was dissolved in Tris-EDTA buffer (Sigma-Aldrich, St Louis, MO, USA).
Total mRNAs was extracted using TRI-REAGENT® (Sigma-Aldrich, St Louis, MO, USA) solution, according to the manufacturer's instruction. The nucleic acid quality was tested by using NanoDrop 2000 (Thermo Scientific) and the absorbance ratio was measured at 260/230 and 260/280 um.

3.3 cDNA AND REAL TIME PCR

One microgram of total mRNAs was reverse transcribed using SensiFAST® cDNA Synthesis Kit (Bioline, London, UK) according to the manufacturer's instruction, dissolved in 20μL of nuclease-free water (Qiagen, Hilden, Germany). All PCR real time experiments were performed three times on a 7500 Real Times PCR System (Applied Biosystems, Foster City, CA, USA) using the SYBR® Green-detection system (Roche, Penzberg, Germany). The complete list of oligonucleotides used is reported in Table II.

3.4 PROTEIN EXTRACTION AND WESTERN BLOT ANALYSIS

Cells lysis was carried out using RIPA-Buffer (Sigma-Aldrich, St Louis, MO, USA) and protein concentration was determined by Bio-Rad protein assay. Equal amounts of denatured proteins were subjects to SDS PAGE 10% polyacrylamide gel. Proteins were visualized using ECL substrate (Euroclone, Milano, Italy) and ECL chemiluminescence film (Fujifilm®). Phospho S1981 ATM (Abcam, Cambridge, UK) normalized using as reference total ATM (Abcam, Cambridge, UK) protein and normalized to β-actin (Sigma-Aldrich, St Louis, MO, USA) as loading control. Western blot bands were normalized to β-actin with Image J software.

3.5 CHROMATIN IMMUNOPRECIPITATION

HeLa cells were starved, as indicated in the legend of the Figures. Cells were fixed using formaldehyde at final concentration of 1%. The reaction was quenched by adding 125mM glycine.
Nuclei were isolated using a lysis buffer (Proteinase inhibitor cocktail, 10 mM Tris pH 8.0, 10 mM NaCl, NP40 0,2%, PMSF 1%) and fragmented by sonication (Bioruptor® Pico Sonicator, Diagenode, Ougrèe, Belgium). An aliquot of each sample was used as INPUT, and the remaining fraction was precipitated using phosphor-γH2AX antibody (Cell Signaling, Danvers, MA, USA). All samples were processed using a ChIP assay kit (Upstate Biotechnology, Lake Placid, NY, USA) according to the manufacturer's instructions. Real Time PCR was used to quantify the immune-precipitated DNA and the data were normalized to the input. All values represent the average of at least three independent experiments.

3.6 FLOW CYTOMETRY ANALYSIS

Cells were harvested and fixed with 70% cold ethanol and PBS solution in a ratio 9:1 at 4°C overnight. After was in PBS, the cells were incubated in 500 µl of staining solution (20 µg/mL propidium iodide; 0,1-0,2 mg/mL RNaseA; TRITON 0,1%) at room temperature for 30 min. The samples were analyzed with the FACSCAN (BD, Heidelberg, Germany) and the cell cycle distribution was analyzed with the software WINMDI.

3.7 MeDIP ASSAY

Cells were treated as indicated in legends of the Figures. A total of ~2,6 × 10^6 cells were harvested and genomic DNA extracted as described above. 7,7 µg of total genomic DNA was digested in 100 µl for 16 h AT 37° with restriction endonuclease mix containing 30 U each of Eco RI, Hind III, Hpa II (Roche, Penzberg, Germany), phenol/chloroform extracted, ethanol precipitated and re-suspended in 50 µl of TE buffer (10 mM Tris pH 8.0, 1 mM EDTA). An aliquot (1/10) of digested DNA was used as input control to determine DNA concentration and digestion efficiency. Remaining DNA was diluted in 500 µl of immunoprecipitation buffer (0.15% SDS, 1% Triton X-100, 150 mM NaCl, 1 mM EDTA pH 8.0, 0.5 mM EGTA pH 8.0, 10 mM Tris pH 8.0, 0.1% BSA, 7 mM NaOH) and incubated at 95°C for 10 min before the immunoprecipitation with 5 µg of 5-methyl cytosine antibody (Abcam, Cambridge, UK). As a control, 5 µg of normal mouse IgG (Santa Cruz, Dallas, TX, USA) was included.
Samples were, then, extracted with phenol-chloroform-isoamyl alcohol, ethanol precipitated and re-suspended in TE buffer. All samples were analyzed by Real Time PCR.

3.8 BISULFITE TREATMENT AND AMPLICON LIBRARY PREPARATION

We converted 2 µg of genomic DNA in genomic bisulfite DNA using according EZ DNA Methylation Kit (Zymo Research, Irvine, CA, USA) and eluted in 50µl of d-H_2O following the manufacturer's instruction. An amplicon library of bisulfite treated DNA was generated performing a double step PCR. In the first PCR reaction, fragment of size about 500-550bp were amplified. The second PCR reaction is performed in order to add a nucleotide tag, using specific primers containing multiplexing indices and Illumina® sequencing adapters. The first PCR was performed using a "FastStart High Fidelity PCR System"(Roche, Penzberg, Germany) at the following thermo cycle conditions: one cycle at 95°C for 2 min followed by 30 cycles at 95°C for 30 sec, at TM 50°C for 45 sec, at 72°C for 60 sec, followed by a final extension step at 72°C for 10 min. Reactions were performed in 20 µl total volumes: 2 µl 10x reaction buffer, 1 µl of 10 mM dNTP mix, 1 µl of 4 µM forward and reverse primers, 3.6 µl MgCl2 25 mM, 2-4 µl bisulfite template DNA, 0.25 µl FastStart Taq, and d-H2O up to a final volume of 30 µl. Five microliters of the first PCRs were used to check the product size on 1.5% agarose gel.

A purification step using 20µl of AMPure purification magnetic Beads (Beckman-Coulter, Brea, CA, USA) following the manufacturer's instructions, was performed before the second PCR to eliminate small DNA fragments. The second PCR was performed in a 50 µl final volume: 5 µl 10x reaction buffer, 2.5 µl of 10 mM dNTP mix, 5 µl forward and reverse "Nextera XT" primers (Illumina, SanDiego, CA, USA), 6 µl MgCl2 25 mM, 5 µl of first PCR product, 0.4 µl FastStart Taq, and d-H2O up to a final volume of 50 µl. Thermo-cycle settings were: one cycle at 95°C for 2 min followed by 8 cycles at 95°C 30s, 55°C for 40 sec, 72°C for 40 sec, followed by a final extension step at 72°C for 10 min.

3.9 SEQUENCE ANALYSIS

All paired–ends reads (minimum overlapping residue = 40) obtained from Illumina Miseq sequencer platform were matched together using PEAR tool. The quality filtered was obtained using as threshold a mean of PHREAD score at least 33. FASTQ assembled reads were converted to FASTA format using PRINSEQ tool. To analyze the methylation status of each amplicon was used a pipeline software (Amplimethprofiler) freely available at *https://sourceforge.net/projects/amplimethprofiler* (Scala, 2016).

3.10 ANTIBODIES

The following antibodies were used in this study: Anti-5-methylcytosine ab10805 (Abcam); Anti-ATM (phosphor S1981) ab81292 (Abcam); Anti-ATM ab199726 (Abcam); Anti-gamma H2A.X (phospho S139) ab2893 (Abcam); Anti-beta Actin sc-47778 (Santa Cruz Biotechnology); Normal mouse IgG sc-2025 (Santa Cruz Biotechnology).

3.11 STATISTICAL ANALYSIS

All data are presented as mean ± standard deviation in at least three experiments in triplicate (n=9 or greater). Statistical significance between groups was determined using Student's t test on Excel program (matched pairs test or unmatched test were used as indicated in figure legends).

TABLE II

Primers for mRNA

18s fw	5'-GCG CTA CAC TGA CTG GCT C-3'
18s rv	5'-CAT CCA ATC GGT AGT AGC GAC-3'
CDKN2A fw	5'-AGT TAC GGT CGG AGG CCG AT-3'
CDKN2A rv	5'-TGG AGC AGC AGC AGC TCC-3'
CDKN2B fw	5'-ACT AGT GGA GAA GGT GCG ACA-3'
CDKN2B rv	5'-TAG GTT CCA GCC CCG ATC C-3'
CDKN2A-ARF fw	5'-CTA CTG AGG AGC CAG CGT CTA-3'
CDKN2A-ARF rv	5'-CTG CCC ATC ATC ATG ACC T-3'
CDKN1A fw	5'-GCT GGT GGC TAT TTT GTC CT-3'
CDKN1A rv	5'-CAT GGG TTC TGA CGG ACA T-3'
α-SMA fw	5'-CTG TTC CAG CCA TCC TTC AT-3'
α-SMA rv	5'-TCA TGA TGC TGT TGT AGG TGG T-3'

Primers for ChIP

CDKN2A fw	5'-AGA GTA GTC AAC GCA GTG TC-3'
CDKN2A rv	5'-TGA GAG CTG ATC CCA GTC TTG-3'
CDKN2B fw	5'-ATT AGC CTT GGC TTT ACT GG-3'
CDKN2B rv	5'-GGC AAA GAA TTC CGT TTT CAG C-3'
CDKN2A-ARF fw	5'-GAG CCG TTC CGA GAT CTT GG-3'
CDKN2A-ARF rv	5'-CCC CTT AAC TGC AGA CTG G-3'
CDKN1A fw	5'-ATG TGT CCA GCG CAC CAA CG-3'
CDKN1A rv	5'-AGC TCA GCG CGG CCC TGA TAT AC-3'

Primers for Bisulfite

CDKN2A fw	5'-TTT TTA GAG GAT TTG AGG GAT AGG-3'
CDKN2A rv	5'-CTA CCT AAT TCC AAT TCC CCT ACA AAC-3'

4. RESULTS

4.1 TRANSCRIPTIONAL REGULATION OF CDKN2A/B GENES DURING CELL CYCLE

CDKN2A/B suppressor genes are located on chromosome 9p21 in INK4-ARF locus. These genes are transcriptionally repressed in many tumors but the biological mechanism leading to silencing is not known.
To dissect the mechanism of transcriptional silencing of these genes, we focused our efforts on the regulation of $p15^{INK4B}$ and $p16^{INK4A}$ p14ARF genes during cell cycle progression.
Hela cells were used as model system to investigate the regulation of expression of $p15^{INK4B}$ $p16^{INK4A}$ p14ARF during cell cycle progression. We starved HeLa cells from fetal bovine serum (FBS) for several periods of time and serum was re-added to allow the entry of the cells into cycle.
The mRNA analysis by qPCR of $p15^{INK4B}$ $p16^{INK4A}$ p14ARF and p21/CDKN1A genes is shown in Fig. 5. The mRNAs levels of $p15^{INK4B}$ $p16^{INK4A}$ and p14ARF increased after 2 hours of starvation. Under these culture conditions p21/CDKN1A mRNA did not change significantly.

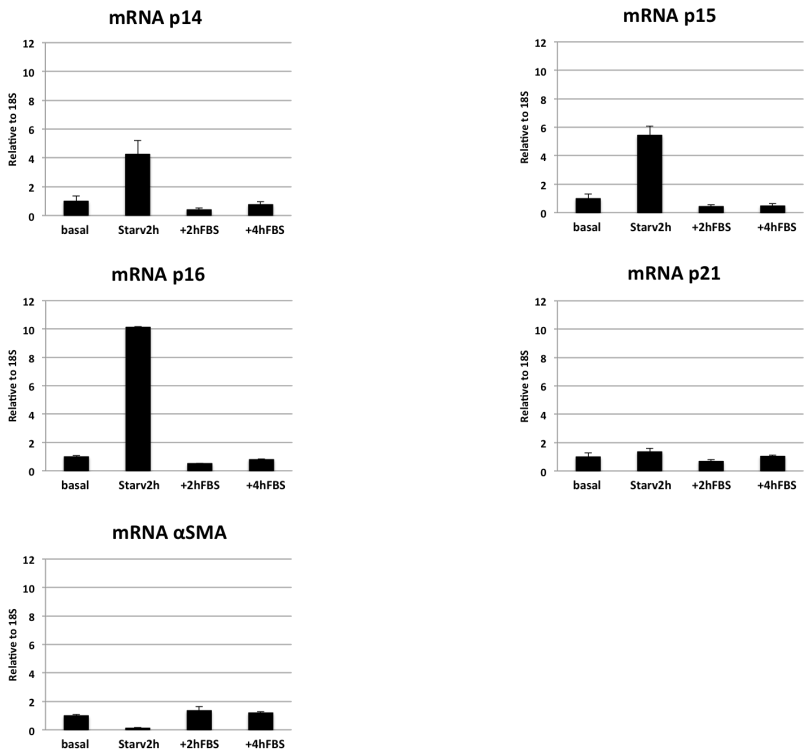

Figure 5: Induction of p15^{INK4B} p16^{INK4A} and p14ARF mRNA By Serum Starvation. Analysis of CDKN2A-B and control genes by RT-PCR. Cells were subjected to FBS starvation for 2 h. The serum was added for 6 h and total RNA extracted and analyzed by qPCR with the appropriate primers indicated in M&M. Each column represents the average value of experiments in triplicate (2 technical and 1 biological replicates).

The data shown in Fig. 5 suggest that p15^{INK4B} p16^{INK4A} and p14ARF expression is higher in G0 and early G1 cells and is repressed in S phase. To demonstrate that the expression of INK4-ARF locus genes is regulated during the phases of the cell cycle, we performed a cell cycle analysis by flow cytometry. As for mRNA analysis, cells were starved and re-induced to entry the cycle by adding the serum for different periods of time (2 and 4 h). Figure 6 shows that after 2 h starvation the majority of cells are in G0/G1 phase and this corresponds to the higher expression levels of p15^{INK4B} p16^{INK4A} and p14ARF. Induction of cell cycle entry reduces dramatically p15^{INK4B} p16^{INK4A} and p14ARF expression. Under the same conditions p21 mRNA levels do not change (Fig. 5).

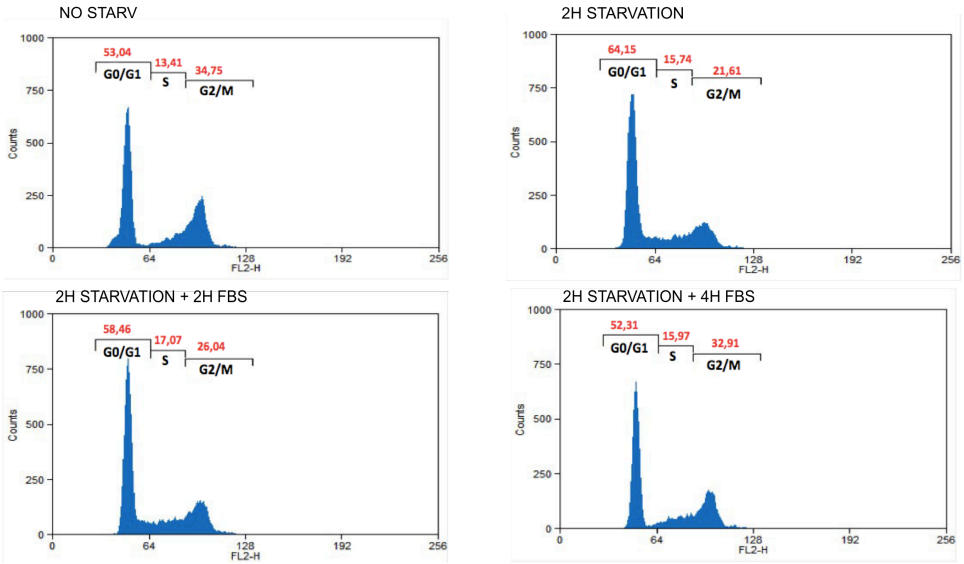

Figure 6: Cell Cycle Progression of Hela Cells Before, During And After Serum Starvation. The experiment was performed as described in figure 5, cells were fixed and stained with propidium iodide prior to analysis in a FACSCAN. The graphs show the relative DNA content (x axis) versus cell number (y axis). Red numbers indicate the percent of cells in each cell cycle step. Each experiment was performed at least in triplicate.

We conclude that serum starvation for 2 hour is able to induce $p15^{INK4B}$ $p16^{INK4A}$ p14ARF and synchronize the cells in G0/G1.

4.2 DNA DAMAGE SIGNATURES AT CDKN2A-B GENE PROMOTERS.

Three replication origins are present at the INK4-ARF locus. Specifically, the three mapped replication origins are close to transcriptional start sites of $p15^{INK4B}$ and $p16^{INK4A}$ p14ARF genes (Fig. 7) (Dellino *et al.,* 2013).

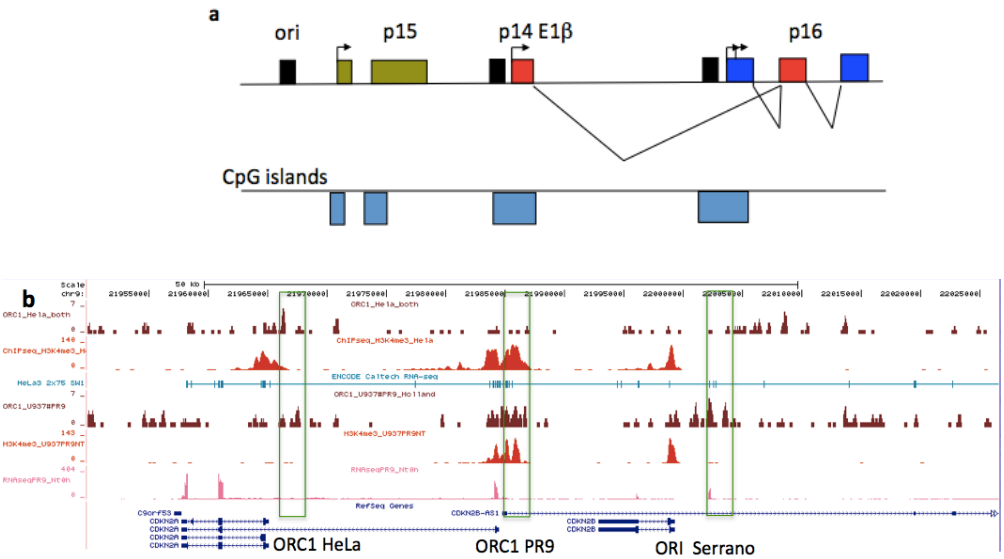

Figure 7: The INK4-ARF Locus. Panel a shows the CDKN2A-B locus: the upper line and boxes represent the replication origins (ori, black), the exons encoding CDKN2B (p15, green); CDKN2A-ARF (p14, red) and CDKN2A (p16, blue); the lower line with blue boxes indicates the location of the CpG islands. Panel b shows the replication origins (indicated by a green box) mapped in PG and Hela cells by I Dellino et al., in Genome Res., 2013 doi: 10.1101/gr.142331.112.

Since CDKN2A-B genes are induced by starvation and repressed when the cells enter the cycle (Fig. 5-6) it is possible that the rapid cycles of transcription induction-repression (G0-G1) and replication activation (G1-S), occurring at the same DNA regions, may generate local DNA damage by physical interference between RNA and DNA polymerases.

To better investigate the consequences of switching on and off p14ARF $p15^{INK4B}$ $p16^{INK4A}$ transcription, we performed a Chromatin Immunoprecipitation (ChIP) assay with antibodies to phospho-γ-H2aX protein (pγ-H2AX), a marker of DNA double strand breaks (Kuo and Yang, 2008) in HeLa cells subjected to cycles of starvation.

Fig. 8 shows that pγ-H2AX signal accumulates at the promoter region of CDKN2A-B genes selectively when S1 phase begins (Fig. 6). Under the

same conditions p2/CDKN1A promoter did not show any evidence of pγ-H2AX accumulation (Fig. 8).

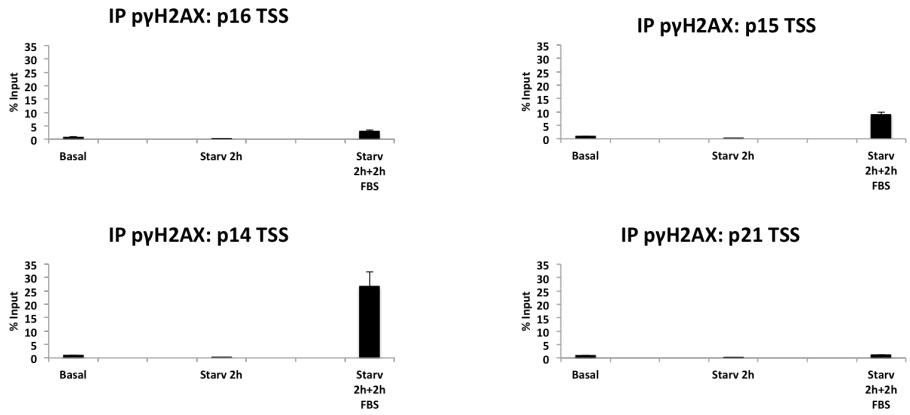

Figure 8: DNA Damage Signature At CDKN2A-B Promoters. The experiment was performed as described in Figure 1. Cells were fixed by paraformaldehyde solution and the chromatin was analyzed by ChIP assay using pγH2AX antibody. All primers were designed in order to match the (TSS) transcriptional start site region (a range of 1000bp from the coding DNA sequences or CDS). Each experiment was performed at least in triplicate.

To obtain an independent evidence of DNA damage under conditions of 2h starvation+ 2h serum (2+2), we performed a western blot with anti phospho-ATM antibodies. The starvation cycles (2+2) induce phospho-ATM and confirm the DNA damage found at the CDKN2A-B promoters by pγ-H2AX accumulation (Fig. 9). The topoisomerase II inhibitor etoposide was used as positive control of DNA damage (Fig.9).

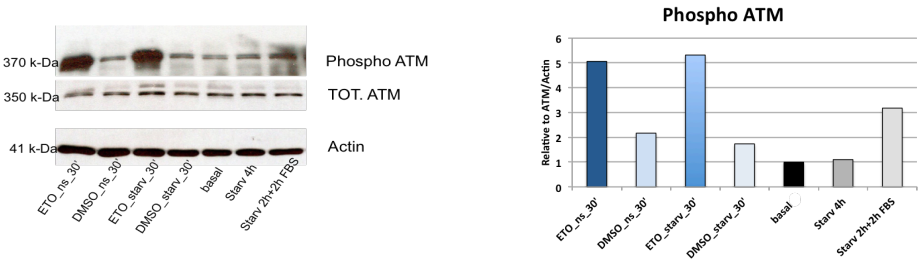

Figure 9: DNA Damage Occurs In Hela Starved Cells After FBS Administration. Immunoblot analysis of phosphoATM and total ATM in cells exposed to etoposide or starved as indicated at the bottom of the gel (A). B shows the quantification of the bands relative to total ATM or to beta actin. Each experiment was performed at least in triplicate.

4.3 INHIBITION OF DNA POLYMERASE OR OF RNA POLYMERASE REDUCES γH2AX ACCUMULATION AT CDKN2A/B PROMOTERS

The data shown above suggest that interference of DNA polymerase at the onset of S phase with RNA polymerase still engaged at the CDKN2A-B promoters, might be the actual cause of DNA damage signatures found under conditions of short cycles of starvation and serum stimulation (2+2). If this is the case, inhibition of DNA or RNA polymerases should be able to reduce significantly pγ-H2AX accumulation. To this end, we performed a chromatin immunoprecipitation experiment with pγH2aX antibodies interrogating $p16^{INK4A}$ promoter and using two polymerases inhibitors, α-amanitin (Gong *et al.*, 2004) and aphidicolin (Sheaff *et al.*, 1991). Fig. 10 shows that during starvation there is a significant increase of pγ-H2AX accumulation in cells exposed to aphidicolin, whereas under conditions of maximal pγ-H2AX accumulation (2+2) both drugs, aphidicolin and α-amanitin, significantly reduced the accumulation of the DNA damage marker. The effects of aphidicolin in G0, most likely is due to inhibition of DNA repair in G0 (Waters, 1981). It is worth noting that aphidicolin inhibits DNA synthesis but does not induce damage *per se* in the absence of other factors, such as oxidative stress (Fig.10) (Venkatachalam *et al.,* 2017).

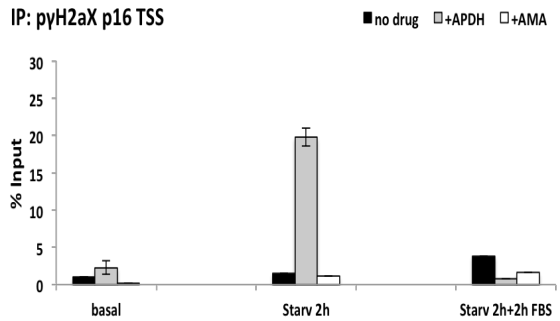

Figure 10: DNA & RNA Polymerase Inhibitors Increase DNA Damage At CDKN2A Promoter. The experimental procedure was the same as in figure 3. The inhibitors were present into the media for the times indicated. Aphidicolin and α-Amanitin, respectively 1μg/mL and 2,5μM final concentration. Each experiment was performed at least in triplicate.

The treatment with aphidicholin did not reduce the $p16^{INK4A}$ mRNA levels following 2 h serum starvation instead it induced it (Fig. 11). α-amanitin inhibited, as expected, the accumulation of $p16^{INK4A}$ mRNA in starved cells (Fig. 11).

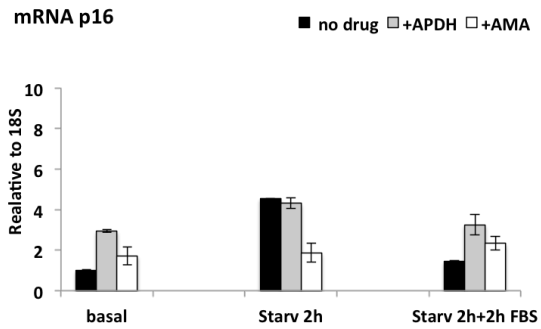

Figure 11: Aphidicholin Does Not Modify The Levels Of CDKN2A mRNA In Starved And Re-Started Cells. The starvation time and drugs treatments are the same as in Fig.9. Each experiment was performed at least in triplicate.

4.4 METHYLATION ASSOCIATED WITH DNA DAMAGE AT $p16^{INK4A}$ PROMOTER

Our previous data indicate that DNA damage and repair are associated with de novo DNA methylation (Russo et al., 2016). It is likely that DNA damage at p16INK4A promoter eventually might result in de novo methylation.
The data shown above demonstrate that rapid cycles of starvation and serum re-addition induce DNA damage at p16INK4A gene promoter (Fig. 8). DNA damage signatures are reduced by inhibiting DNA or RNA polymerases (Fig. 10). We repeated the experiment by starving the cells with a same protocol (2+2) and measured the extent of DNA methylation by using the anti methyl CpG antibody (MeDIP) to immunoprecipitate the p16INK4A promoter DNA. Fig. 12 shows that: 1. aphidicholin and a-amanitin increase the methylation signal at the p16INK4A promoter under basal conditions. Inhibition of transcription reduces methylCpGs turnover due to Tet-hydroxymethylation of CpGs (Blattler and Farnham, 2013); 2. 2 h starvation reduces the methylation induced by a-amanitin, because p16INK4A transcription was induced by starvation (Fig.5 and 6). The stimulatory effect on methylation by aphidicholin in starved cells seems to be a consequence of inhibition of DNA repair (Lee et al., 2012). The most striking stimulation of methylation is visible in cells that accumulate DNA damage (2+2) (Fig. 8). The cells undergoing rapid cycles of starvation and serum stimulation accumulate high levels of g-H2AX and increase the CpG methylation signal (Fig. 12).
Collectively these data support the idea that rapid stimulation of replication and transcription cycles facilitates collisions between DNA polymerase assembled at initiating replication forks and RNA polymerase recruited to the promoter, which happens to be close to a firing replication origin. Eventually,

the repair of the double strand break marks the site with de novo methylation (Russo et al., 2016).

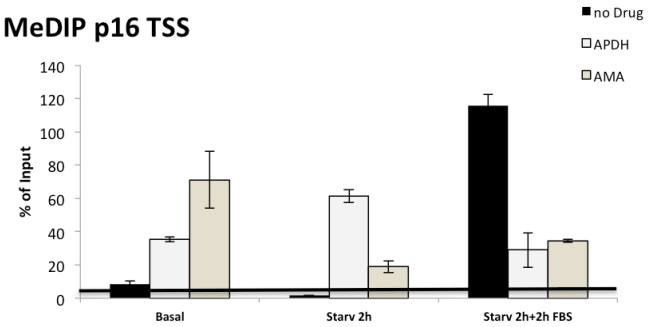

Figure 12: Chromatin Immunoprecipitation of p16^{INK4A} Promoter with Anti Methyl CpG Antibody In Cells Undergoing Rapid Cycles Of Starvation. MeDIP ChIP of the p16^{INK4A} promoter in cells undergoing 2 h starvation and 2 h re-addition of FBS (2+2) in presence and absence of aphidicolin and α-amanitin (as described in Fig. 8 and 10). Each experiment was performed in triplicate.

4.5 METHYLATED CDKN2A ALLELES *IN VIVO* EVOLVE DURING THE PROGRESSION OF ACUTE MYELOID LEUKEMIA

The data shown above suggest a link between DNA damage and methylation of CDKN2A-B genes. Methylation of suppressor genes in cancer may be a consequence of DNA damage generated by DNA and RNA polymerases. Since the methylation profiles are stable and heritable, it is likely that methylated INK4-ARF alleles are under positive selection pressure and may mark successful cancer cells escaping senescence. The analysis of the methylation profiles of p16^{INK4A} may provide a window to track the progressive evolution of cells harboring dominant oncogene mutations
Since loss of p16^{INK4A} gene stabilizes leukemogenesis, specifically AML (Shields *et al.,* 2016), we decided to analyze the methylation profiles of p16^{INK4A} alleles spanning the TSS by deep sequencing of bisulfite DNA extracted from bone marrow (BM) or peripheral blood of three AML patients (A,B and C) during the disease progression. All the sequences were performed on DNA molecules with identical 5' and 3' ends and each sequence was representative of a single chromosome. We define these alleles that vary only by the location of methylated CpGs, epi-alleles. The configuration of several methylated CpGs in a single DNA molecule represents the epigenetic equivalent of the haplotype (epi-haplotype).

In patient A we found a Single Nucleotide Polymorphism SNP (G/T), which has been used to analyze the segregation of methylation with allelic variants. Briefly, the methylated alleles differing only by methylation were considered epialleles and their frequency analyzed in the total cell population.

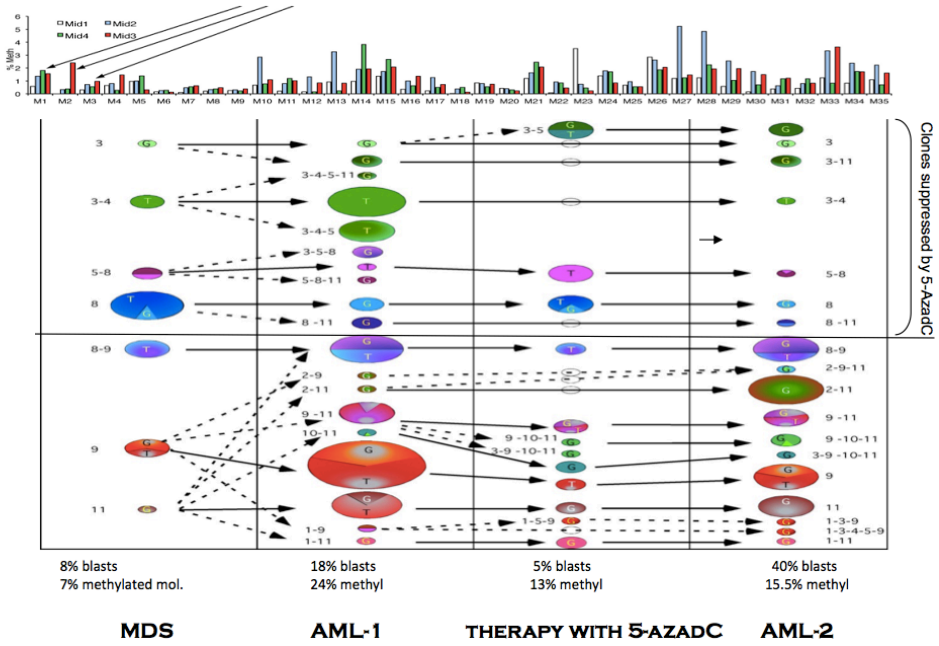

Figure 13: Evolution of p16^{INK4A} **epiallele in the bone marrow cells of Patient A.** The upper inset shows the % methylation of each CpG at the 5' end of p16^{INK4A} gene (35 CpG from -110-to +150 from the transcription start site) the arrows indicate the increase of methylation at specific site in the last step of our analysis. The histogram shows the methylation of the CpGs in each sample (MID1, grey, MID2 blue, MID3 red, MID4, green), samples correspond to MDS, AML-1, AzadC and AML-2, which represent the different stages of the disease: 1-MDS, (Myelodysplastic syndrome, RAEB I); 2-AML-1 indicates the progression 1 year after MDS; 3-AzadC indicates the cytological remission of AML-1, 3 months after therapy with VIDAZA® (75 mg/m2/day subcutaneously for 7 days of a 28-day cycle, 2 cycles); 4-AML-2 is the final stage of the disease 6 months later (after VIDAZA®). In the segment of p16^{INK4A} gene analyzed here, there are 35 CpGs, which have been clustered in 11 groups (the first group of CpGs at the 5' end is marked as 1 and the most 3' end group is indicated as 11). The color of the circles identifies the specific CpGs methylated, while the area of the circles indicates the frequency of each epiallele. G or T in each circle indicates the frequency in the specific group of epialleles (color) of the SNP G/T found in the p16^{INK4A} segment analyzed. The fraction of blasts present in the sample is indicated below the columns along with the fraction of methylated molecules and the date of the sample collection. Mono-methylated molecules were excluded from the analysis.

The histogram at the top of Fig. 13 shows the relative frequency of p16^{INK4A} epialleles. As shown also by others, the distribution of methylated sites is higher at the 5' and 3' borders of the nucleosome. In this specific case, there is a nucleosome signature (the first nucleosome from the TSS) centered on CpG position 19-20 (data not shown and Hinshelwood *et al.,* 2009 and Wong *et al.,* 1999).

Fig. 13 shows the distribution and the map of the most representative epialleles present in the cell population derived from the BM of patient A at different stages of the disease. The sequences are shown as circles, the color identifies the specific methylated CpGs and the size represents the relative frequency of each methylated species in the total population.
At the onset of the disease, MDS (Fig. 13, first column on the left) classified as myelodysplasia (Table I), there are 7 major molecules methylated at the 5' (CpG 1- 6) or 3' (CpG 9-10) end of the $p16^{INK4A}$-I exon. The most frequent methylated molecules are bi or trimethylated and represent approximately 7 to 10% of all molecules sequenced (2 to 10K/sample). The G or T alleles (SNP) are evenly distributed in the epiallelic groups, indicating that no specific selection is applied on this SNP. One year later, MDS evolves into AML (AML-1, in Fig. 13) and there is a clear amplification of the epialelles seen in M in addition to new variants. The similarity of the CpGs locations suggests that new variants originate from previous epialleles that gain 1 or 2 methyl groups. This is also suggested by net gain of methylated molecules, which reach 24% of the total compared to 7% in MDS. Therapy with Vidaza® (5- AzadC), DNMT inhibitor, (Fig. 13 III Column, AzadC) significantly reduces all the clonal families; 1. it eradicates clones (3-4-5, green clones) ; 2. it generates new variants (9-10-11) or (1-5-9); 3. it amplifies older clones (5-8-11). The last stage of the disease corresponding to the relapse, shows a strong positive selection on few clones (Fig. 13, clone 9 - 10-11) indicating that the disease at this stage is mono or oligoclonal (Fig. 13, AML-2). The presence of the G/T SNP greatly facilitates the analysis of the segregation of the epialelles described and confirms the negative (loss) or positive (gain) selection on epialleles during the progression of the disease (Fig. 13). The detailed analysis of the association between the SNPs and the epialleles shows that few original clones (two or three) generate the entire collection of clones that characterize AML-1, AzadC and AML-2 during the progression of the disease. Many clones (Fig.13, clone 3, 3-4, 5-8 and 8) disappear after the therapy and do not evolve (Fig. 13, Aza-dC sensitive clones). Other clones become rampant after the therapy and evolve faster than before therapy (Fig. 13, CpG 2-11). This finding is relevant because 5-AzadC resistant clones were already detectable 6 months before AML-2 (Fig. 13 lower part) when the fraction of blasts was 5% and clinical phenotype was classified as stable remission.
Since this is a dynamic analysis based on the difference in epiallelic frequency, it is important to provide normal or non-evolving controls. To this end we analyzed the distribution of $p16^{INK4A}$ epiallele frequency in several normal BM controls.

Figure 14 shows that the bone marrow of two normal subjects contains several p16 epialleles at very low frequency. We did not detect epialleles at frequency higher than 0.01% (see below).

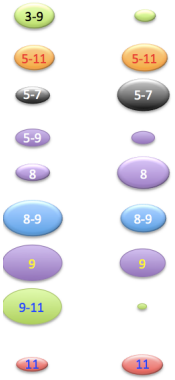

Figure 14: Frequency And Distribution Of Epialleles Of p16^{INK4A} From bone marrow (BM) Of 2 Normal Subjects. Similar epialleles are shown by colored circles; color identifies the specific methylated CpGs and the area indicates the frequency

This suggests that no selection is applied on cells carrying methylated alleles of p16^{INK4A} in the absence of oncogenic mutations.
To extend our observation, we analyzed p16^{INK4A} epialleles in other 2 patients (Fig. 15) one with a myelodysplastic syndrome (patient B) and another presenting an overt myeloid acute leukemia (patient C).

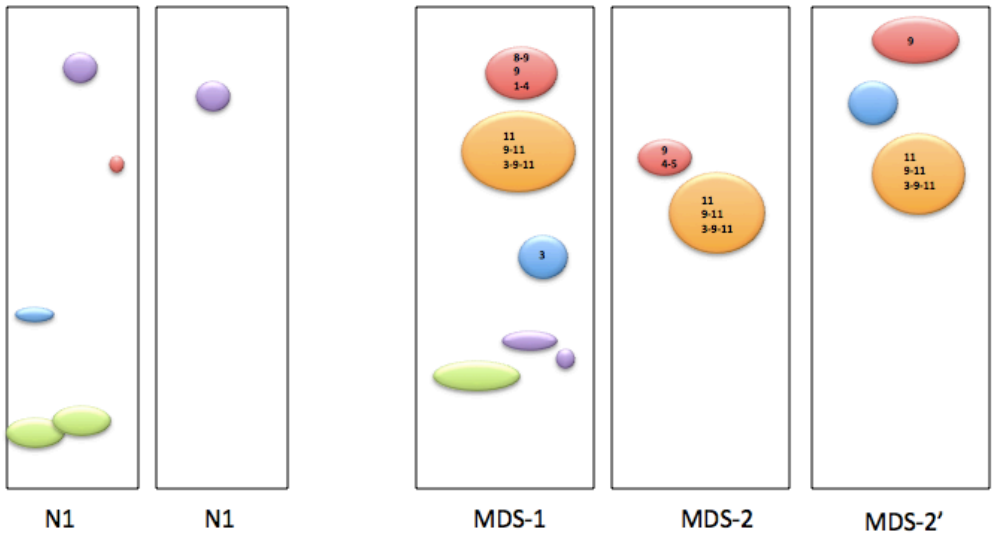

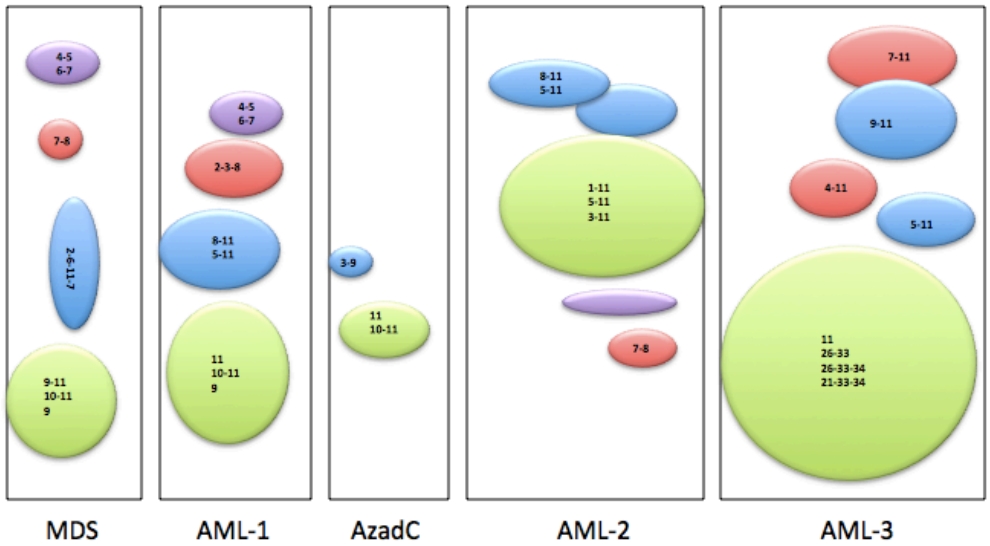

Figure 15: Frequency And Distribution Epialleles p16^{INK4A} in BM Of AML patients (B, upper panel and C, lower panel). The upper panel shows the frequency of epialleles in 2 control BMs, N1-N2 and in the samples of patient B, MDS-1 (myelodysplasia), MDS-2 (3 months after chemotherapy) and MDS-2' (1 year later). The lower panel shows the epiallele frequency in BM samples derived from patient C at the onset of the disease (MDS, myelodysplasia) or overt AML-1, after the therapy with Vidaza® (azadC) or in relapse (AML-2 and 3), respectively.

As in patient A, we found higher frequency epialleles (Fig. 15) methylated in few locations (5' and 3' end of the segment analyzed, see Fig. 7a top inset). Many epialleles were similar to those in the patient A (Fig. 13 and 15, CpG11). The upper panel shows, control BMs (Fig. 15 first 2 columns, N1, N2) and 2 stages of the BM of patient B indicated as MDS-1 (Upper panel, table II B diagnosis) and MDS-2 after therapy (Upper panel, table III-IV, B, remission). The sequence of sample MDS-2' was repeated 1 year after the therapy and no substantial change in the frequency of the major epialleles was detected (Fig. 15, upper panel MDS-2 and MDS-2').

The lower panel in Fig. 15 shows the distribution of epialelles in another set of samples derived from a third patient (Fig. 15, patient C), which shows a dramatic and fast evolution of the epialleles corresponding to the progression of the disease. The samples derive from the initial myelodysplasia (MDS) and from overt AML-1, followed by remission after the demethylating therapy using Vidaza® (AzadC) and relapse (AML-2 and AML-3). As in Fig. 13, there are very similar epialleles that are amplified or hardly eliminated by therapy. Also in this case, we notice that therapy facilitates the amplification of groups of epialleles. In the final stage of the disease (AML-2) 80% of the sequences are represented by 1 clone marked by methylation of CpG 11 group.

These data demonstrate that these $p16^{INK4A}$ epialleles are not *per se* the cause of the amplification or evolution of the tumor, because similar epialleles are present also in not evolving diseases or normal BM (Fig. 15, patient B), but their presence confers a selective advantage to founder clones carrying oncogenic mutations. Remind that a great fraction of mutated oncogene induces senescence, only if $p16^{INK4A}$ is expressed. Since methylation in this region of $p16^{INK4A}$ is frequent, the association of these epialelles with oncogenic clones occurs at high frequency (Qiu *et al.,* 2011). These clones acquire a higher fitness because they exit stably or transiently from senescence and become rampant with the time.

In conclusion, the analysis of $p16^{INK4A}$ epialleles *in vivo* longitudinally in the same patient shows that the $p16^{INK4A}$ epialleles evolve in the 2 AML patients, but not in normal controls. In control samples there are many methylation profiles corresponding to a large variety of epialleles, but their frequency is stable overtime. Also, we wish to note that in patient B the analysis of the epialleles shows that disease (MDS) did not progress and stabilized overtime (Fig. 15, upper panel).

We conclude that the qualitative analysis of methylation profiles $p16^{INK4A}$ epialleles genes not only describes accurately the evolution of AML but can be used to track specific clones and, ultimately, predict chemoresistance.

5. DISCUSSION

5.1 MOLECOLAR COLLISIONS BETWEEN REPLICATION AND TRANSCRIPTION MACHINES ARE SOURCES OF DNA DAMAGE

Everyday, cells are subjected to lesions from exogenous and endogenous sources: continuous exposure of the cells to DNA damaging agents induces degenerative changes and rapid aging. Products of cellular metabolism are also able to induce DNA damage that affects cell fitness similarly to the effects of common environmental agents, such as UV, ionizing radiations or natural/man-made genotoxic chemicals.
The endogenous sources of DNA mutations derive from errors of replication and DNA repair (see for comments Tomasetti *et al.,* 2017). Also, Interference and conflicts between DNA replication and transcription machines, in terms of molecular collisions, has been described in bacteria as potential cause of DSB (French, 1992) (Liu and Alberts, 1995).
In the context of collisions between DNA and RNA polymerases, it is possible to describe two different scenarios: co-directional and head-on collision.

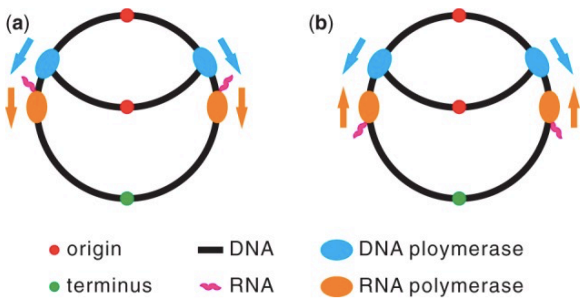

Figure 16: Schematic Representation Of Collision Between DNA And RNA Polymerase Complexes In Bacteria. (a) Co-directional collision occurs when a gene is encoded on the leading strand. (b) Head-on collision occurs when a gene is encoded on the lagging strand.
Adapted from Chen; 2013; doi: 10.1093/gbe/evt193.

The difference in speed of DNA and RNA polymerase in bacteria (Rocha and Danchin, 2003) generates co-directional collisions when the enzymes are working on the leading strand (Fig. 16 a). If the genes are highly transcribed (Merrikh *et al.,* 2011), they became hotspots of co-directional conflicts. If a nick is present on the transcribed strand, DNA polymerase will stop and a DSB will be generated. Repair of the site by HR may leave methylated sites on the template strand (Russo *et al.,* 2016).

On the other hand, when a gene is encoded on the lagging strand, head-on collisions occur (Fig. 16 b) (Chen and Zhang, 2013). The head-on collisions translate in a stop of replication fork progression and replication stress (Merrikh *et al.,* 2011). Pause of replication fork (RFP) by head-on collisions is associated, in mammalian cells, with increase of HR activity at that site (Prado and Aguilera, 2005) in order to prevent genomic instability. The regions of RFP coupled to DNA break formation are known as common fragile sites (CFS) (Helmrich *et al.,* 2011). Also, in these cases HR leaves methylation marks on the repaired segment (Cuozzo *et al.,* 2017; Morano *et al.,* 2014).

5.2 DNA DAMAGE AND DNA METHYLATION

The relation between DNA damage, repair and DNA methylation seems well established. DNA methyltrasferase-I and IIIa-b enzymes are implicated in DNA damage, repair and methylation. DNMT1 is found associated with proliferating cell nuclear antigen (PCNA) during replication and repair (Chuang *et al.,* 1997), and it is required to prevent genomic instability (Chen *et al.,* 1998). How these events were temporally related was discovered later.
C. Cuozzo *et al.* in 2007 and G. Russo *et al.* in 2016, using the DRGFP plasmid developed by M.Jasin (Pierce *et al.,* 1999), demonstrated that DSB and HR induce early transient and stable inheritable changes of local chromatin. Local DNA methylation is essential to stabilize the chromatin changes induced by DSB and HR and transcription also reshapes local DNA methylation following damage and HR. Together, DNA damage and transcription may be ultimately responsible for the high degree of polymorphism of somatic methylation. DNA damage increases in hyperplastic precancerous cells and precedes genomic instability and loss of p53 expression in many tumors (Gorgoulis *et al.,* 2005). Repair of the lesions by HR and methylation generate a pool of cells with different levels of expression of the repaired gene and depending on the function of the gene (oncosuppressor genes, for example) *de novo* DNA methylation induced by damage and repair can confer a inheritable selective advantage.

5.3 METHYLATION OF CDKN2A-B SUPPRESSOR GENES IS A FREQUENT EVENT DURING NEOPLASTIC PROGRESSION

Silencing of CDKN2A-B suppressor genes is a very frequent event during cancer progression. In fact, the expression of these genes, in cells carrying dominant oncogene mutations, induces senescence (Bianchi-Smiraglia and

Nikiforov, 2012). Methylation of DNA may be an important cause of silencing, but is not known what kind of event leads to gene silencing.
Two different models have been proposed. An epigenetic change, such as promoter CpG island hypermethylatyon, can occur randomly at the site of DNA damage. If this modification modifies gene expression then a selective advantage for the modified cell will be forwarded to daughter cells (Hassler and Egger, 2012). This model is essentially stochastic because the DNA modified site is random.
A determinist event, on the contrary, leading to methylation of a specific DNA segment can be induced by oncogene-activated transcriptional factors targeting at the specific site the, *de novo* methyl transferases, DNMT3a or b. There are many examples of oncogenic proteins able to induce silencing of oncosoppressor genes, for example K-RAS. K-RAS directed signalling in colorectal cancer cells switches off INK4-ARF genes. The oncogene activates a zinc finger protein ZNF304 that recruits at the promoters of INK4-ARF genes DNMT1. Targeted DNMT1 induces inheritable local methylation and repression of transcription (Serra *et* al., 2014).
Other oncogenic proteins can trigger similar pathways, for example Myc in lymphoma T cells (Opavsky *et* al., 2007).
The data presented here support both models because DNA methylation is dependent on damage and transcription. The activation or stimulation of transcription and replication are essentially deterministic events because they are induced by specific proteins and factors that recognize specific sequences in the genome; on the other hand, the DNA damage induced at TSS by interference between transcription and replication is stochastic because it depends on the timing and on the chances that DNA and RNA polymerases are present and travelling on the same strand. The stochastic component of methylation is also highlighted by the high polymorphism, which is cell and individual specific.

5.4 DNA METHYLATION AS BAR-CODE TO IDENTIFY AND TRACK SPECIFIC EPIALLELES

The data presented here highlight the variability and the polymorphism of $p16^{INK4A}$ methylated alleles (epialleles). The polymorphism of CpG at TSS of $p16^{INK4A}$ can be detected and measured because deep sequencing of bisulfite-treated DNA was performed on single DNA molecules with the same 5' and 3' ends. In complex populations of cells, such as those found in BM or blood from AML patients, the number of different epialleles in the population defines the frequency and the degree of the methylation-polymorphism (epi-polymorphism). The combination of different epiallele families in an

individual DNA sample can be represented as a bar code that characterizes the individual DNA. During the progression of AML in the 2 patients we have documented changes in the frequency of $p16^{INK4A}$ epialleles, which reflect positive and negative selection exerted on families of epialleles by genetic and epigenetic changes. For example, the demethylating therapy amplified some families of epialleles and reduced others. This conclusion can be drawn only by the analysis of the frequency overtime of each epiallele family (Fig. 13-15). Ultimately, the epigenetic distance between epialleles can be calculated as the difference in methyl CpG location in pairs of samples and the appearance of successful clones can be detected by computing the frequency of epiallele families overtime.

5.5 QUANTITATIVE VS QUALITATIVE DNA METHYLATION ANALYSIS

Nowadays, the limit of the analysis of changes in DNA methylation status and their relationship with cancer progression is due to the lower coverage and to the quantitative assessment of each methylated CpG. The population of bisulfite resistant CpGs does not allow the analysis of single DNA molecules. Pyrosequencing highlights the statistical occurrence of single methylated CpGs in the majority of molecules, but doe not allow the analysis of single molecules with different location of methylated CpGs. These moelcules are described as epialleles similarly to alleles defined by SNPs.
We have applied the same analysis of SNPs to methylCpGs. This approach provides information on alleles differing only by location of methylated CpGs (see Florio et al., 2017).

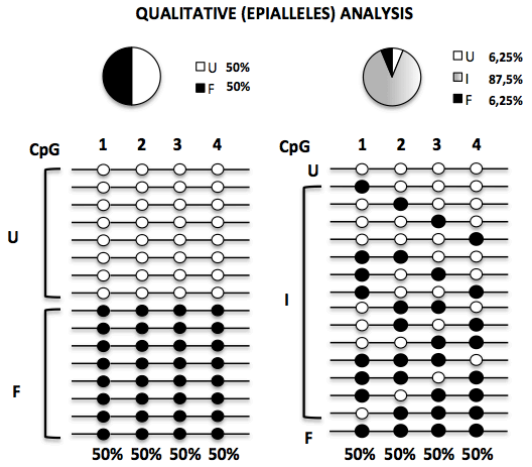

Figure 17: Schematic Representation Of Quantitative VS Qualitative Methylation Analysis Of Epialleles. In the figure 4 GpG are performed by (on the left side) a quantitative and (on the right side) a qualitative analysis where U= un-methylated F= fully-methylated I= intermediate.
Adapted from Florio; 2017; 10.1080/15592294.2016.1260211

As shown in Fig. 17, the quantitative approach overlooks the heterogeneity of a population dividing it only into two major groups of epialleles, while the qualitative analysis allows the identification of families of epialleles and greatly reduces the heterogeneity of methylation. Since cancer cells are highly heterogeneous (Gay *et al.,* 2016), this type of qualitative analysis of methylation applied to a complex population of cells can reduce heterogeneity and identify clones.
The analysis of $p16^{INK4A}$ epialleles in AML reported here shows that the heterogeneity of epialleles is only apparent because we can identify and tarck the same clones overtime during the progression of the disease.
The presence/absence of epialleles and their increase/decrease of frequency after a treatment give to us an estimation of the efficiency of the treatment and eventually suggest us to move to other drugs.

6. CONCLUSIONS

The methylation of the promoter of oncosoppressor genes is a common event during cancer progression and the data presented here provide a possible explanation of the molecular mechanism underlying gene silencing.
Progressive CpG methylation at $p16^{INK4A}$ promoter region is a direct consequence of endogenous damage. $p16^{INK4A}$ silenced cells overcome the senescence barrier and increase the fitness overtime. The progressive accumulation of methyl groups at the TSS of $p16^{INK4A}$ further improves the fitness of cell clones and favors the neoplastic progression. *In vivo* we identify several epialleles of $p16^{INK4A}$ gene and overtime in 2 cases of AML we document a selective amplification of certain types of epialleles, which are resistant to the demethylating therapy and are further amplified at the disease relapse.
These data offer an explanation for cancer heterogeneity, but especially provide an effective and precise approach to monitor the patients during the therapy.

7. REFERENCES

Besson A, Dowdy SF, Roberts JM. CDK inhibitors: cell cycle regulators and beyond. Dev Cell. 2008 Feb;14(2):159-69. doi:10.1016/j.devcel.2008.01.013.

Bianchi-Smiraglia A, Nikiforov MA. Controversial aspects of oncogene-induced senescence. Cell Cycle. 2012 Nov 15;11(22):4147-51. doi: 10.4161/cc.22589.

Blattler A, Farnham PJ. Cross-talk between site-specific transcription factors and DNA methylation states. J Biol Chem. 2013 Nov 29;288(48):34287-94. doi: 10.1074/jbc.R113.512517. Epub 2013 Oct 22. Review.

Chen RZ, Pettersson U, Beard C, Jackson-Grusby L, Jaenisch R. DNA hypomethylation leads to elevated mutation rates. Nature. 1998 Sep 3;395(6697):89-93.

Chen X, Zhang J. Why are genes encoded on the lagging strand of the bacterial genome? Genome Biol Evol. 2013;5(12):2436-9. doi: 10.1093/gbe/evt193.

Cheng M, Olivier P, Diehl JA, Fero M, Roussel MF, Roberts JM, Sherr CJ. The p21(Cip1) and p27(Kip1) CDK 'inhibitors' are essential activators of cyclin D-dependent kinases in murine fibroblasts. EMBO J. 1999 Mar 15;18(6):1571-83.

Chim CS, Liang R, Tam CY, Kwong YL. Methylation of p15 and p16 genes in acute promyelocytic leukemia: potential diagnostic and prognostic significance. J Clin Oncol. 2001 Apr 1;19(7):2033-40.

Christiansen DH, Andersen MK, Pedersen-Bjergaard J. Methylation of p15INK4B is common, is associated with deletion of genes on chromosome arm 7q and predicts a poor prognosis in therapy-related myelodysplasia and acute myeloid leukemia. Leukemia. 2003 Sep;17(9):1813-9.

Chuang LS, Ian HI, Koh TW, Ng HH, Xu G, Li BF. Human DNA-(cytosine-5) methyltransferase-PCNA complex as a target for p21WAF1. Science. 1997 Sep 26;277(5334):1996-2000.

Cuozzo C, Porcellini A, Angrisano T, Morano A, Lee B, Di Pardo A, Messina S, Iuliano R, Fusco A, Santillo MR, Muller MT, Chiariotti L, Gottesman ME, Avvedimento EV. DNA damage, homology-directed repair, and DNA methylation. PLoS Genet. 2007 Jul;3(7):e110. Erratum in: PLoS Genet. 2017 Feb 10;13(2):e1006605.

Dellino GI, Cittaro D, Piccioni R, Luzi L, Banfi S, Segalla S, Cesaroni M, Mendoza-Maldonado R, Giacca M, Pelicci PG. Genome-wide mapping of human DNA-replication origins: levels of transcription at ORC1 sites regulate origin selection and replication timing. Genome Res. 2013 Jan;23(1):1-11. doi: 10.1101/gr.142331.112.

Demetrius L. Of mice and men. When it comes to studying ageing and the means to slow it down, mice are not just small humans. EMBO Rep. 2005 Jul;6 Spec No:S39-44.

Denicourt C, Dowdy SF. Cip/Kip proteins: more than just CDKs inhibitors. Genes Dev. 2004 Apr 15;18(8):851-5.

Diede SJ, Yao Z, Keyes CC, Tyler AE, Dey J, Hackett CS, Elsaesser K, Kemp CJ, Neiman PE, Weiss WA, Olson JM, Tapscott SJ. Fundamental differences in promoter CpG island DNA hypermethylation between human cancer and genetically engineered mouse models of cancer. Epigenetics. 2013 Dec;8(12):1254-60. doi: 10.4161/epi.26486.

Drexler HG. Review of alterations of the cyclin-dependent kinase inhibitor INK4 family genes p15, p16, p18 and p19 in human leukemia-lymphoma cells. Leukemia. 1998 Jun;12(6):845-59.

Esteller M. CpG island hypermethylation and tumor suppressor genes: a booming present, a brighter future. Oncogene. 2002 Aug 12;21(35):5427-40.

Ferreira WA, Araújo MD, Anselmo NP, de Oliveira EH, Brito JR, Burbano RR, Harada ML, Borges Bdo N. Expression Analysis of Genes Involved in the RB/E2F Pathway in Astrocytic Tumors. PLoS One. 2015 Aug 28;10(8):e0137259. doi: 10.1371/journal.pone.0137259.

Florio E, Keller S, Coretti L, Affinito O, Scala G, Errico F, Fico A, Boscia F, Sisalli MJ, Reccia MG, Miele G, Monticelli A, Scorziello A, Lembo F, Colucci-D'Amato L, Minchiotti G, Avvedimento VE, Usiello

A, Cocozza S, Chiariotti L. Tracking the evolution of epialleles during neural differentiation and brain development: D-Aspartate oxidase as a model gene. Epigenetics. 2017 Jan 2;12(1):41-54. doi: 10.1080/15592294.2016.1260211.

French S. Consequences of replication fork movement through transcription units in vivo. Science. 1992 Nov 20;258(5086):1362-5.

Furukawa Y, Kikuchi J, Nakamura M, Iwase S, Yamada H, Matsuda M. Lineage-specific regulation of cell cycle control gene expression during haematopoietic cell differentiation. Br J Haematol. 2000 Sep;110(3):663-73.

Gartel AL, Radhakrishnan SK. Lost in transcription: p21 repression, mechanisms, and consequences. Cancer Res. 2005 May 15;65(10):3980-5.

Gartel AL, Tyner AL. Transcriptional regulation of the p21((WAF1/CIP1)) gene. Exp Cell Res. 1999 Feb 1;246(2):280-9.

Gay L, Baker AM, Graham TA. Tumour Cell Heterogeneity. F1000Res. 2016 Feb 29;5. pii: F1000 Faculty Rev-238. doi: 10.12688/f1000research.7210.1. eCollection 2016. Review.

Gil J, Peters G. Regulation of the INK4b-ARF-INK4a tumour suppressor locus: all for one or one for all. Nat Rev Mol Cell Biol. 2006 Sep;7(9):667-77.

Gong XQ, Nedialkov YA, Burton ZF. Alpha-amanitin blocks translocation by human RNA polymerase II. J Biol Chem. 2004 Jun 25;279(26):27422-7.

Gorgoulis VG, Vassiliou LV, Karakaidos P, Zacharatos P, Kotsinas A, Liloglou T, Venere M, Ditullio RA Jr, Kastrinakis NG, Levy B, Kletsas D, Yoneta A, Herlyn M, Kittas C, Halazonetis TD. Activation of the DNA damage checkpoint and genomic instability in human precancerous lesions. Nature. 2005 Apr 14;434(7035):907-13.

Harper JW, Adami GR, Wei N, Keyomarsi K, Elledge SJ. The p21 Cdk-interacting protein Cip1 is a potent inhibitor of G1 cyclin-dependent kinases. Cell. 1993 Nov 19;75(4):805-16.

Hassler MR, Egger G. Epigenomics of cancer - emerging new concepts. Biochimie. 2012 Nov;94(11):2219-30. doi: 10.1016/j.biochi.2012.05.007. Epub 2012 May 17.

Helman A, Klochendler A, Azazmeh N, Gabai Y, Horwitz E, Anzi S, Swisa A, Condiotti R, Granit RZ, Nevo Y, Fixler Y, Shreibman D, Zamir A, Tornovsky-Babeay S, Dai C, Glaser B, Powers AC, Shapiro AM, Magnuson MA, Dor Y, Ben-Porath I. p16(Ink4a)-induced senescence of pancreatic beta cells enhances insulin secretion. Nat Med. 2016 Apr;22(4):412-20. doi: 10.1038/nm.4054.

Helmrich A, Ballarino M, Tora L. Collisions between replication and transcription complexes cause common fragile site instability at the longest human genes. Mol Cell. 2011 Dec 23;44(6):966-77. doi: 10.1016/j.molcel.2011.10.013.

Hinshelwood RA, Melki JR, Huschtscha LI, Paul C, Song JZ, Stirzaker C, Reddel RR, Clark SJ. Aberrant de novo methylation of the p16INK4A CpG island is initiated post gene silencing in association with chromatin remodelling and mimics nucleosome positioning. Hum Mol Genet. 2009 Aug 15;18(16):3098-109. doi: 10.1093/hmg/ddp251.

Jenkins NC, Liu T, Cassidy P, Leachman SA, Boucher KM, Goodson AG, Samadashwily G, Grossman D. The p16(INK4A) tumor suppressor regulates cellular oxidative stress. Oncogene. 2011 Jan 20;30(3):265-74. doi: 10.1038/onc.2010.419.

Kazanets A, Shorstova T, Hilmi K, Marques M, Witcher M. Epigenetic silencing of tumor suppressor genes: Paradigms, puzzles, and potential. Biochim Biophys Acta. 2016 Apr;1865(2):275-88. doi: 10.1016/j.bbcan.2016.04.001.

Kim WY, Sharpless NE. The regulation of INK4/ARF in cancer and aging. Cell. 2006 Oct 20;127(2):265-75.

Kuo LJ, Yang LX. Gamma-H2AX - a novel biomarker for DNA double-strand breaks. In Vivo. 2008 May-Jun;22(3):305-9.

Lafargue A, Degorre C, Corre I, Alves-Guerra MC, Gaugler MH, Vallette F, Pecqueur C, Paris F. Ionizing radiation induces long-term senescence in endothelial cells through mitochondrial respiratory complex II dysfunction and superoxide generation. Free Radic Biol Med. 2017 Jul;108:750-759. doi: 10.1016/j.freeradbiomed.2017.04.019.

Landan G, Cohen NM, Mukamel Z, Bar A, Molchadsky A, Brosh R, Horn-Saban S, Zalcenstein DA, Goldfinger N, Zundelevich A, Gal-Yam EN, Rotter V, Tanay A. Epigenetic polymorphism and the stochastic formation of differentially methylated regions in normal and cancerous tissues. Nat Genet. 2012 Nov;44(11):1207-14. doi: 10.1038/ng.2442.

LaPak KM, Burd CE. The Molecular Balancing Act of p16INK4a in Cancer and Aging. Molecular cancer research : MCR. 2014;12(2):167-183. doi:10.1158/1541-7786.MCR-13-0350.

Lee B, Morano A, Porcellini A, Muller MT. GADD45α inhibition of DNMT1 dependent DNA methylation during homology directed DNA repair. Nucleic Acids Res. 2012 Mar;40(6):2481-93. doi: 10.1093/nar/gkr1115.

Lee EY, Muller WJ. Oncogenes and tumor suppressor genes. Cold Spring Harb Perspect Biol. 2010 Oct;2(10):a003236. doi: 10.1101/cshperspect.a003236.

Li H, Collado M, Villasante A, et al. The Ink4/Arf locus is a barrier for iPS
reprogramming. Nature.2009;460(7259):11361139.doi:10.1038/nature08290.

Li S, Garrett-Bakelman FE, Chung SS, Sanders MA, Hricik T, Rapaport F, Patel J, Dillon R, Vijay P, Brown AL, Perl AE, Cannon J, Bullinger L, Luger S, Becker M, Lewis ID, To LB, Delwel R, Löwenberg B, Döhner H, Döhner K, Guzman ML, Hassane DC, Roboz GJ, Grimwade D, Valk PJ, D'Andrea RJ, Carroll M, Park CY, Neuberg D, Levine R, Melnick AM, Mason CE. Distinct evolution and dynamics of epigenetic and genetic heterogeneity in acute myeloid leukemia. Nat Med. 2016 Jul;22(7):792-9. doi: 10.1038/nm.4125.

Liu B, Alberts BM. Head-on collision between a DNA replication apparatus and RNA polymerase transcription complex. Science. 1995 Feb 24;267(5201):1131-7.

Liu Y, Johnson SM, Fedoriw Y, Rogers AB, Yuan H, Krishnamurthy J, Sharpless NE. Expression of p16(INK4a) prevents cancer and promotes aging in lymphocytes. Blood. 2011 Mar 24;117(12):3257-67. doi: 10.1182/blood-2010-09-304402.

Luo G, Santoro IM, McDaniel LD, Nishijima I, Mills M, Youssoufian H, Vogel H, Schultz RA, Bradley A. Cancer predisposition caused by elevated mitotic recombination in Bloom mice. Nat Genet. 2000 Dec;26(4):424-9.

Merrikh H, Machón C, Grainger WH, Grossman AD, Soultanas P. Co-directional replication-transcription conflicts lead to replication restart. Nature. 2011 Feb 24;470(7335):554-7. doi: 10.1038/nature09758.

Miyake S, Nagai K, Yoshino K, Oto M, Endo M, Yuasa Y. Point mutations and allelic deletion of tumor suppressor gene DCC in human esophageal squamous cell carcinomas and their relation to metastasis. Cancer Res. 1994 Jun 1;54(11):3007-10.

Morano A, Angrisano T, Russo G, Landi R, Pezone A, Bartollino S, Zuchegna C, Babbio F, Bonapace IM, Allen B, Muller MT, Chiariotti L, Gottesman ME, Porcellini A, Avvedimento EV. Targeted DNA methylation by homology-directed repair in mammalian cells. Transcription reshapes methylation on the repaired gene. Nucleic Acids Res. 2014 Jan;42(2):804-21. doi: 10.1093/nar/gkt920.

Opavsky R, Wang SH, Trikha P, Raval A, Huang Y, Wu YZ, Rodriguez B, Keller B, Liyanarachchi S, Wei G, Davuluri RV, Weinstein M, Felsher D, Ostrowski M, Leone G, Plass C. CpG island methylation in a mouse model of lymphoma is driven by the genetic configuration of tumor cells. PLoS Genet. 2007 Sep;3(9):1757-69. Epub 2007 Aug 16.

Otto T, Sicinski P. Cell cycle proteins as promising targets in cancer therapy. Nat Rev Cancer. 2017 Jan 27;17(2):93-115. doi: 10.1038/nrc.2016.138.

Pierce AJ, Johnson RD, Thompson LH, Jasin M. XRCC3 promotes homology-directed repair of DNA damage in mammalian cells. Genes Dev. 1999 Oct 15;13(20):2633-8.

Prado F, Aguilera A. Impairment of replication fork progression mediates RNA polII transcription-associated recombination. EMBO J. 2005 Mar 23;24(6):1267-76.

Qiu W, Sahin F, Iacobuzio-Donahue CA, Garcia-Carracedo D, Wang WM, Kuo CY, Chen D, Arking DE, Lowy AM, Hruban RH, Remotti HE, Su GH. Disruption of p16 and activation of Kras in pancreas increase

ductal adenocarcinoma formation and metastasis in vivo. Oncotarget. 2011 Nov;2(11):862-73.

Rangarajan A, Weinberg RA. Opinion: Comparative biology of mouse versus human cells: modelling human cancer in mice. Nat Rev Cancer. 2003 Dec;3(12):952-9. doi: 10.1038/nrc1235.

Rich JN, Zhang M, Datto MB, Bigner DD, Wang XF. Transforming growth factor-beta-mediated p15(INK4B) induction and growth inhibition in astrocytes is SMAD3-dependent and a pathway prominently altered in human glioma cell lines. J Biol Chem. 1999 Dec 3;274(49):35053-8.

Rocha EP, Danchin A. Gene essentiality determines chromosome organisation in bacteria. Nucleic Acids Res. 2003 Nov 15;31(22):6570-7.

Russo G, Landi R, Pezone A, Morano A, Zuchegna C, Romano A, Muller MT, Gottesman ME, Porcellini A, Avvedimento EV. DNA damage and Repair Modify DNA methylation and Chromatin Domain of the Targeted Locus: Mechanism of allele methylation polymorphism. Sci Rep. 2016 Sep 15;6:33222. doi: 10.1038/srep33222.

Sadikovic B, Al-Romaih K, Squire JA, Zielenska M. Cause and consequences of genetic and epigenetic alterations in human cancer. Curr Genomics. 2008 Sep;9(6):394-408. doi: 10.2174/138920208785699580.

Sánchez-Beato M, Sáez AI, Martínez-Montero JC, Sol Mateo M, Sánchez-Verde L, Villuendas R, Troncone G, Piris MA. Cyclin-dependent kinase inhibitor p27KIP1 in lymphoid tissue: p27KIP1 expression is inversely proportional to the proliferative index. Am J Pathol. 1997 Jul;151(1):151-60.

Scala G, Affinito O, Palumbo D, Florio E, Monticelli A, Miele G, Chiariotti L, Cocozza S. ampliMethProfiler: a pipeline for the analysis of CpG methylation profiles of targeted deep bisulfite sequenced amplicons. BMC Bioinformatics. 2016 Nov 25;17(1):484.

Serra RW, Fang M, Park SM, Hutchinson L, Green MR. A KRAS-directed transcriptional silencing pathway that mediates the CpG island methylator phenotype. Elife. 2014 Mar 12;3:e02313. doi: 10.7554/eLife.02313

Serrano M, Lee H, Chin L, Cordon-Cardo C, Beach D, DePinho RA. Role of the INK4a locus in tumor suppression and cell mortality. Cell. 1996 Apr 5;85(1):27-37.

Shah MY, Vasanthakumar A, Barnes NY, Figueroa ME, Kamp A, Hendrick C, Ostler KR, Davis EM, Lin S, Anastasi J, Le Beau MM, Moskowitz IP, Melnick A, Pytel P, Godley LA. DNMT3B7, a truncated DNMT3B isoform expressed in human tumors, disrupts embryonic development and accelerates lymphomagenesis. Cancer Res. 2010 Jul 15;70(14):5840-50. doi: 10.1158/0008-5472.CAN-10-0847.

Sheaff R, Ilsley D, Kuchta R. Mechanism of DNA polymerase alpha inhibition by aphidicolin. Biochemistry. 1991 Sep 3;30(35):8590-7.

Sherr CJ. Ink4-Arf Locus in Cancer and Aging. Wiley interdisciplinary reviews Developmental biology. 2012;1(5):731-741. doi:10.1002/wdev.40.

Shields BJ, Jackson JT, Metcalf D, Shi W, Huang Q, Garnham AL, Glaser SP, Beck D, Pimanda JE, Bogue CW, Smyth GK, Alexander WS, McCormack MP. Acute myeloid leukemia requires Hhex to enable PRC2-mediated epigenetic repression of Cdkn2a. Genes Dev. 2016 Jan 1;30(1):78-91. doi: 10.1101/gad.268425.115.

Skalska L, White RE, Parker GA, Turro E, Sinclair AJ, Paschos K, Allday MJ. Induction of p16(INK4a) is the major barrier to proliferation when Epstein-Barr virus (EBV) transforms primary B cells into lymphoblastoid cell lines. PLoS Pathog. 2013 Feb;9(2):e1003187. doi: 10.1371/journal.ppat.1003187. Epub 2013 Feb 21. Erratum in: PLoS Pathog. 2013 Mar; 9(3): doi:10.1371/annotation/2c4b89c1-6d4a-4bf3-9467-9367227d7e74.

Starostina NG, Kipreos ET. Multiple degradation pathways regulate versatile CIP/KIP CDK inhibitors. Trends Cell Biol. 2012 Jan;22(1):33-41. doi: 10.1016/j.tcb.2011.10.004.

Teofili L, Martini M, Di Mario A, Rutella S, Urbano R, Luongo M, Leone G, Larocca LM. Expression of p15(ink4b) gene during megakaryocytic differentiation of normal and myelodysplastic hematopoietic progenitors. Blood. 2001 Jul 15;98(2):495-7.

Thiagalingam S, Laken S, Willson JK, Markowitz SD, Kinzler KW, Vogelstein B, Lengauer C. Mechanisms underlying losses of heterozygosity in human colorectal cancers. Proc Natl Acad Sci U S A. 2001 Feb 27;98(5):2698-702. Epub 2001 Feb 13.

Tomasetti C, Li L, Vogelstein B. Stem cell divisions, somatic mutations, cancer etiology, and cancer prevention. Science. 2017 Mar 24;355(6331):1330-1334. doi: 10.1126/science.aaf9011.

Urbach D, Lupien M, Karagas MR, Moore JH. Cancer heterogeneity: origins and implications for genetic association studies. Trends Genet. 2012 Nov;28(11):538-43. doi: 10.1016/j.tig.2012.07.001.

Venkatachalam G, Surana U, Clément MV. Replication stress-induced endogenous DNA damage drives cellular senescence induced by a sub-lethal oxidative stress. Nucleic Acids Res. 2017 Jul 31. doi: 10.1093/nar/gkx684.

Waters R. Aphidicolin: an inhibitor of DNA repair in human fibroblasts. Carcinogenesis. 1981;2(8):795-7.

Whelan AJ, Bartsch D, Goodfellow PJ. Brief report: a familial syndrome of pancreatic cancer and melanoma with a mutation in the CDKN2 tumor-suppressor gene. N Engl J Med. 1995 Oct 12;333(15):975-7.

Wong DJ, Foster SA, Galloway DA, Reid BJ. Progressive region-specific de novo methylation of the p16 CpG island in primary human mammary epithelial cell strains during escape from M(0) growth arrest. Mol Cell Biol. 1999 Aug;19(8):5642-51.

Zhang J, Lindroos A, Ollila S, Russell A, Marra G, Mueller H, Peltomaki P, Plasilova M, Heinimann K. Gene conversion is a frequent mechanism of inactivation of the wild-type allele in cancers from MLH1/MSH2 deletion carriers. Cancer Res. 2006 Jan 15;66(2):659-64.

Zhang Y, Xiong Y, Yarbrough WG. ARF promotes MDM2 degradation and stabilizes p53: ARF-INK4a locus deletion impairs both the Rb and p53 tumor suppression pathways. Cell. 1998 Mar 20;92(6):725-34